



DEPARTMENT OF CYBERNETICS

DIGIW PROJECT

Dynamic Modelling of Heart Rate During Wheelchair Propulsion

Author: Sina Øilo Tenold

December, 2022

Contents

List of Figures	iii
List of Tables	v
1 Introduction	2
1.1 Background & Motivation	2
1.2 Data Collection	2
1.2.1 Participants	3
1.2.2 Experiments	3
1.2.3 Equipment	5
1.3 Research Objectives	5
2 Theory	6
2.1 Biological background	6
2.1.1 Heart rate dynamics	6
2.1.2 IPAQ	6
2.2 System identification	7
2.2.1 First order model	7
2.2.2 Second order model	7
2.3 Numerical optimization	7
2.3.1 Broyden–Fletcher–Goldfarb–Shanno algorithm	8
2.4 Least squares estimation	8
2.5 Measurements of performance	8
2.5.1 Coefficient of determination: R^2	8
2.6 Fourier transform	9
2.7 Correlation analysis	9
3 Method	10
3.1 Pre-processing and Data cleaning	10
3.1.1 Missing data	11
3.1.2 Smoothing	12
3.1.3 Input construction	12
3.2 System identification	13
3.2.1 Data organization	13
3.2.2 Cost function	14

3.3	Numerical optimization	14
3.4	Model structures	15
3.4.1	First order linear model	15
3.4.2	First order nonlinear models	15
3.4.3	Second order linear model	16
3.4.4	Second order nonlinear models	16
4	Results	18
4.1	First order linear model	18
4.1.1	First order nonlinear model	20
4.1.2	Second order linear model	20
4.1.3	Second order nonlinear model	22
4.2	Model summary	22
5	Discussion	25
5.1	Model performances	25
5.1.1	Input	25
5.1.2	Order	28
5.1.3	Linearity	30
5.1.4	Smoothing	31
5.1.5	Generalizability	31
5.2	Demographic correlations	32
5.3	Challenges	32
5.4	Further research	32
6	Conclusion	34
	References	35

List of Figures

1	Timeline of a single testing day, note that the incline and the speeds of the interval stages vary from day to day	4
2	Visualisation of experimental setup of wheelchair attached to a rig on the treadmill. Figure taken from (Cappozzo, 2022)	4
3	Raw HR signal from one experiment day from polar sensor located around a participant's chest with annotations indicating rest-periods	10
4	Raw continuous HR signal from polar sensor located on the participant's chest.	11
5	Raw HR signal from one full experiment day for one participant displaying long periods of missing records.	12
6	Raw HR data and data smoothed with Fourier transform. Data stems from one full experiment day for one participant. 'th' is the threshold used to determine which frequencies to remove from the signal	13
7	Input signal constructed as a single source based on a combination of speed and incline of the treadmill. The y-axis gives the magnitude of the input and has no direct physical interpretation in terms of units.	14
8	Input signal constructed as two separate sources, one is the speed [km/h] and the other is the incline [%] of the treadmill	15
9	Concatenated HR of all test days for a single participant. Missing signals were imputed with the mode, and the mode has been subtracted from all points.	16
10	HR-signal from one stage for one participant showing similar response to a first order system	16
11	HR-signal from one stage for one participant showing similar response to a second order system with integrating effect	17
12	First order linear model fit to one participant for an entire experiment day	18
13	Heatmap of correlations between demographic variables and parameters obtained for the first order linear models	18
14	First order linear models based on separated input, fit to one participant over all experiment days	19
15	Heatmap of correlations between demographic variables and parameters obtained for the first order linear models with separated input	19
16	Parameters obtained from the first order linear model, with separated input when fit to the smoothed data, plotted against characteristics of each participant	21
17	First order nonlinear model, with single input fit to a participant over all days	22
18	Heatmap of correlations between demographic variables and parameters obtained from the first order nonlinear model with single input	22
19	First order nonlinear model, with the input separated into two, fit to one participant over all experiment days	23
20	Heatmap of correlations between demographic variables and parameters obtained from the first order nonlinear model with separated input	23
21	Parameters of the first order nonlinear model with separated input based on the smoothed data, plotted against physical properties of each participant	23

22	Second order linear model fit to one participant over all experiment days	24
23	Heatmap of correlations between demographic variables and parameters obtained from a second order linear model	24
24	Second order linear model, with input separated into two fit to one participant over all experiment days	24
25	Heatmap of correlations between demographic variables and parameters obtained from a second order linear model with separate input	25
26	Parameters of the second order linear model, with separated input, with separated input, plotted against physical properties of each participant	26
27	Second order nonlinear models fit to one participant over all three experiment days	27
28	Heatmap of correlations between demographic variables and parameters obtained from second order nonlinear model with single input	27
29	Second order nonlinear model, based on separated input and fit to one participant over all experiment days	27
30	Heatmap of correlations between demographic variables and parameters obtained from second order nonlinear model with separated input	28
31	Parameters of the second order nonlinear model with separated input, based on smoothed HR-signal, plotted against physical properties of each participant	29
32	First and second order nonlinear model, based on separated input and fit to one participant over all experiment days. Plotted together for comparison.	30

List of Tables

1	Summary of the characteristics of the participants	3
2	The speeds and inclines for three testing days with different incline [%] and speed [km/h] on the treadmill.	4
3	MET values	6
4	Table of parameters and fit statistics for all models, with the optimization done on the raw HR-signal. Separated into AB and MWU and averaged over all participants. Models marked as "sep", is based on the separated input signal.	25
5	Table of parameters and fit statistics for all models, with the optimization done on the smoothed version of the HR-signal. Separated into AB and MWU and averaged over all participants. Models marked as "sep", is based on the separated input signal.	28
6	IPAQ correlations between AB-participants and parameters of different models, averaged over all AB participants	31

Abstract

The following thesis was written as part of the Digital Wheelchair Project. Which is a cross-sectional study aiming to create a wearable device for manual wheelchair users. With the capability to objectively track physical activity and estimate energy expenditure to empower them to lead more active lifestyles. This thesis used system identification and numerical optimization to find a mathematical model for heart rate dynamics as a response to propelling in a wheelchair at known speed and incline. Thereafter, an attempt was made to find correlations between demographic variables of the participants and the parameters of the identified models as an initial step towards individualisation of the models.

Sammendrag

Denne oppgaven ble skrevet som del av "the Digital Wheelchair Project". Dette er en tverrfaglig studie med mål om å utvikle en smartklokke for rullestolbrukere. Den skal kunne objektivt gjenkjenne fysisk aktivitet og estimere energiforbruk som et hjelpemiddel for å øke den fysiske aktiviteten i dagliglivet deres. Oppgaven har brukt systemidentifikasjon og numerisk optimering til å identifisere matematiske modeller for pulsdynamikk som en respons til å rulle en rullestol ved kjent hastighet og stigning. Deretter ble det forsøkt å finne korrelasjoner mellom ulike demografiske variable og de estimerte parameterne i modellene som et initielt steg mot individualisering av en slik model.

1 Introduction

This thesis was written as part of the Digital Wheelchair (DigiW) project. A cross-sectional study with the long term goal of developing a wearable device to promote physical activity (PA) amongst manual wheelchair-users (MWU). The project was motivated by comparative inactivity to the general population, the subsequent risk of life-style diseases (Weil et al., 2002) and the low performance of existing wearable devices for this population (Moreno et al., 2020).

1.1 Background & Motivation

Physical Activity (PA) is defined as any "any bodily movement produced by skeletal muscle that substantially increases energy expenditure" (Kesaniemi et al., 2001) and it is closely linked to both mental and physical health. A systematic review found that adults with higher levels of PA have lower all-cause mortality, and incidences of lifestyle diseases such as cardiovascular diseases, obesity, diabetes and certain forms of cancer (Kesaniemi et al., 2001). Moreover, increased PA also reduces symptoms of both depression and anxiety (Paluska and Schwenk, 2000).

The World Health Organization estimated in 2010 that about 1% of the world's total population, which was roughly 65 million people at the time, were in need of wheelchairs (Organization, n.d.). Due to wheelchair-user's (WCU) limited mobility and movement options individuals in wheelchair are prone to living sedentary lifestyles, with lower levels of PA than the general population (Collins et al., 2010; Warms et al., 2008). It is important to consider the heterogeneity of WCU and the vast differences between their lifestyle possibilities and choices due to different underlying conditions. However, on a general basis, movement and muscle involvement is mainly limited to the upper-body for these individuals. In addition to fewer muscles involved in daily life, muscles in the upper body are smaller and thus expend less energy. Consequently, WCU experience a lower metabolic-rate during activity, but also a lower resting metabolic rate (RMR), which in sedentary AB contribute upwards of 80% of the total daily energy expenditure (EE). (Nightingale et al., 2017) Especially, with regards to the obesity-risk, the lower metabolic rate and energy-expenditure poses an issue for WCU. This also invalidates methods used to convert PA into EE in AB-individuals (Nightingale et al., 2017). As a consequence of WCUs overall lower levels of PA, WCUs have a higher probability of experiencing the aforementioned negative effects of limited PA. They are more than three times as likely to suffer from chronic-diseases, such as those mentioned earlier (Tsang et al., 2017). A cross-sectional study performed in Netherlands also found individuals with mobility impairments to have 10 year lower life-expectancy than able-bodied (AB). It is important to account for risk factors in their underlying diseases, however, the study found that six of the years could be explained by lifestyle differences due to limited mobility (I.M. et al., 2011).

Measurement methods with the capacity of accurately measuring the EE, such as indirect calorimetry or doubly-labelled water, are too expensive and impractical for use in free-living situations outside a laboratory (Nightingale et al., 2017). On the other hand there exists a range of wearable devices today that perform well for the ambulatory population, however their accuracy in estimating EE for WCU is significantly lower and are generally not suitable for this purpose (Tsang et al., 2017).

The combination of everything described above is what motivated the DigiW project. The development of algorithms that can accurately and objectively track PA and measure EE in WCU based on multiple sensors on the wheelchair itself and the user empowering them to lead more physically active lives.

1.2 Data Collection

This section presents the data collection process as it has been conducted at NTNU Research Center for Elite Sports (Granåsen Toppidrettssenter) in Trondheim, Norway. Researchers from the DigiW project were responsible for the experimental design, participant recruitment and execution of the experiments. Both healthy able-bodied (AB) participants and manual wheelchair-users

(MWU) have participated in the study so far, their demographic is presented further in Section 1.2.1. The conducted experiments were standardized indoor experiments of wheelchair propulsion on a motorized treadmill with fixed inclines and speeds. The experiment was designed to gather physiological information about the participants at rest, and during wheelchair propulsion of submaximal and maximal efforts, a detailed description of the setup and procedure is provided in Section 1.2.2. Since the experiments were part of a bigger project with multiple research-directions a wide range of sensors were combined in the data-collection, information on relevant equipment and sensors can be found in Section 1.2.3.

1.2.1 Participants

As of 18.12.22, there were 40 participants in the study. 20 of whom are healthy able-bodied participants (AB) that serve as a control group. The remaining 20 participants are manual wheelchair-users (MWU), MWU are a subsection of WCU who manually propel their own wheelchair. The research in this paper is based on data collected from all the 20 AB-participants and the 6 first MWU-participants. The demographic of the study is shown in Table 1.

Table 1: Summary of the characteristics of the participants

Group	Gender	Number	Age	Body Mass (kg)	Height (cm)	Body mass index (BMI) (kg/m ²)
AB	Male	11	33 ± 11	81.9 ± 11.2	183.5 ± 8.2	24.3 ± 2.3
	Female	9	34 ± 11	67.0 ± 7.9	167.3 ± 5.3	24.0 ± 2.6
	Total	20	33 ± 11	75.2 ± 11.4	176.2 ± 9.9	24.2 ± 2.4
MWU	Male	5	38 ± 16	80.0 ± 17.2	180.8 ± 12.5	24.3 ± 3.7
	Female	1	23 ± 0	58.9 ± 0	156 ± 0	24.2 ± 0
	Total	6	35.5 ± 17	76.5 ± 17.6	176.7 ± 15.1	24.3 ± 3.3

Special consideration had to be taken to the heterogeneity of the MWU-group in the study. Although, this might not be reflected in their demographic, there are large variances in body-composition and function within this group. They have a variety of types and severities of motor- and sensory-dysfunction. Three participants suffer from spinal cord injuries (SCI), whereas the remaining three suffer from syndromes affecting the nervous system and/or connective tissue in the body, such as Cerebral Palsy (CP) and Ehlers Danlos (EDS) (Disease Control and Prevention, 2022; NHS, 2022). None of the participants have amputations or missing limbs. Different injuries/syndromes cause vastly different degrees of function-levels, and the same syndrome may also embody itself completely differently in two individuals. This lead to the participants having different degrees of dependence on their wheelchair (and other aids) in their daily life and thereby different prerequisites when performing the experiment. Heterogeneity in the MWU-group must be considered in the analysis of the data and interpretation of the results.

This study includes the data collected from 20 AB who serve as the control group in the full project and 6 MWU. The AB participants have no specified previous experience with wheelchair-use. Inclusion of the 6 MWU was chosen despite the lack of complete data for the entire MWU-group due to a desire to investigate the generalizability of results from AB to MWU.

1.2.2 Experiments

All participants, both the control group consisting of AB, and the MWU, have contributed with testing on three separate days. The most important aspect to ensure consistency between test days is the physical state of the participant, a range of requirements were enforced to ensure this. Therefore, there was a minimum period of 24-hours between each test day, for proper recovery. All test days for each individual participant were completed within a span of three weeks, so that the participant had similar physical fitness on all test days. Sessions were scheduled at the same time of the day, to reduce the variability in the diurnal rhythm (Khemila et al., 2022). Moreover, the

Table 2: The speeds and inclines for three testing days with different incline [%] and speed [km/h] on the treadmill.

Incline	Day 1 (0.5)		Day 2 (2.5)		Day 3 (5.0)	
	Men	Women	Men	Women	Men	Women
Stage 1	4	3	3	2	2	1
Stage 2	6	5	4	3	3	2
Stage 3	8	7	5	4	4	3

participants were asked to arrive at the test in a 2-hour fasted state, and without having performed high-intensity training in the last 24 hours.

On the first test day, general demographic information about the participant was collected. This included height, body-mass, gender and specifics about their disability, such as its severity and ASIA score (Kirshblum et al., 2011). Participants answered the International Physical Activity Questionnaire (IPAQ) (IPAQ, 2004) to assess physical activity. A DXA-scan was also performed of the MWU participants at St.Olav’s Hospital on a separate occasion.

Each test day proceeded as shown in Figure 1. All days started with standard physiological measurements at rest. This involved a 10-minute resting period in which the patient laid down, and sequentially another 10-minute rest in an upright sitting position.

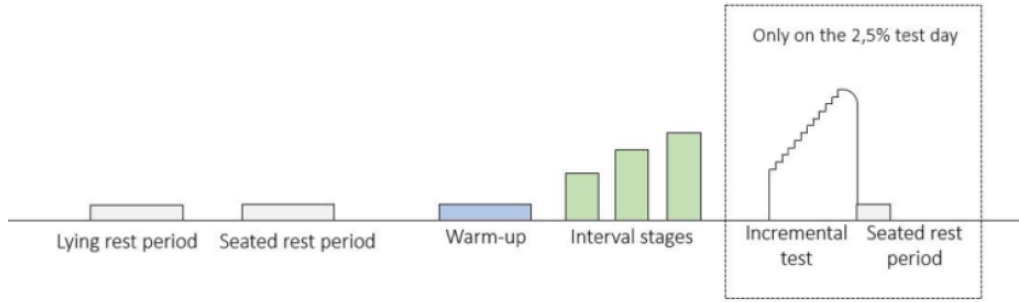


Figure 1: Timeline of a single testing day, note that the incline and the speeds of the interval stages vary from day to day

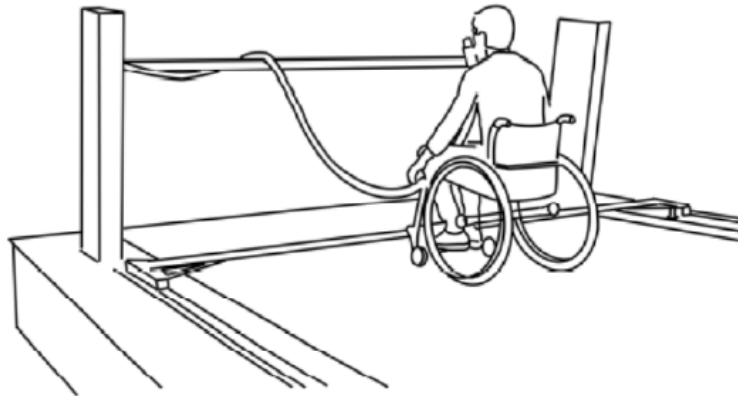


Figure 2: Visualisation of experimental setup of wheelchair attached to a rig on the treadmill. Figure taken from (Cappozzo, 2022)

After the resting measurements the participant sat in the wheelchair. For each test day, the treadmill was fixed to one of the following inclines: 0.5, 2.5 or 5.0%, each of which had a corresponding set of speeds the participant was asked to propel at. Combinations of incline and speed for each day can be found in Table 2. Which order the participant performed the different incline-speed combination was randomly determined. The participants performed a five minute warm-up and habituation on the treadmill at a chosen speed to familiarize themselves with the setup. The participant was instructed to aim for a rating of perceived exertion (RPE) of 7-9 on the Borg scale (Borg, 1982) after this phase. After this, the participant performed the three submax interval stages, hereafter simply referred to as stages. These were four minute intervals, not intended to push the participant beyond their maximal respiratory- or muscular capacities. A resting period of two-three minutes between each stage was enforced. The speeds are given by Table 2. If a participant at anytime was unable to keep up with the set speed, the stage was stopped immediately. For the experiment day where the incline is set to 2.5%, an incremental test followed the three interval stages. This test was intended to test the participant's maximal capacity. The speed increased every minute until the participant reached failure, then the speed was reduced to that before the last increase and the participant continued until exhaustion.

1.2.3 Equipment

The setup is shown in Figure 2. Either a standard wheelchair or the participant's own, in the case of MWU, was used. The wheelchair was attached to a rig on the treadmill which allowed for smooth movement along the rails of the treadmill and prohibited sideways drifting. The HR was measured by a Polar chest strap, connected to Polar M400 HR monitor watch (Polar Electro Oy, Finland). EE was measured by Vyntus ergospirometer (Vyntus CPX, Vyaire, Medical GmbH, Germany) connected to the participant through a fitted face mask. Blood pressure was measured after each of the initial rest periods and blood lactate was measured from ear-lobe after each stage. Moreover, Qualisys motion capture system was used for motion capturing, and accelerometers and inertial measurement units (IMUs) were attached to the wheelchair, the data collected by these instruments are used in other parts of the project and are not included in the scope of this thesis.

1.3 Research Objectives

The research in this project aimed to find a dynamical model structure to track and estimate HR during wheelchair propulsion. The goal was to find out under which conditions and assumptions the model works. Previous attempts at this have been focused on finding models for interval stages in isolation (Cappozzo, 2022), in this thesis the aim was to find a model that can describe all stages and test days by the same structure and parameters. The motivation behind this was the thought that each individual might inhibit a fixed set of parameters that describe their response to input of given intensities, which can then be used in non-standardized settings.

Subsequently, the aim was to find out how much information this model structure may provide on the correlations among relevant estimated parameters. Lastly, some evaluations had to be made on how confident we can be about the knowledge we may extract from the model structure. The research was limited to the controlled case with the speed and incline of propulsion as known variables.

The thesis was written from a control engineering perspective and the mathematical models were found through numerical optimization of systems described through differential equations. Beyond the scope of this project, the models found here can be used to further make models of the EE and find correlations of the parameters between the two.

Primary objective:

Identify model structures for estimating the HR when wheeling at a known speed and incline.

Secondary objectives:

Analyse the goodness of fit and generalizability of the identified models and parameters.

Analyse the possibilities for individualizing the models by investigating the correlations.

Table 3: MET values

Intensity	Values [METs]
Walking	3.3
Moderate PA	4.0
Vigorous PA	8.0

2 Theory

2.1 Biological background

Due to the nature of the experiments this thesis is based on, a certain level of knowledge of the physiological concepts relating to PA and HR is required. The necessary biological concepts for understanding the methods and results in this thesis are presented in the following sections.

2.1.1 Heart rate dynamics

Heart rate (HR) is typically measured in beats per minute (bpm). During exercise the body has an increased circulatory demand, thereby the HR increases to meet the demands of the body during activity (Patel, 2022). The dynamics of this HR-increase, and subsequent -decrease, is dependent upon a range of physiological factors. These are environmental factors, such as temperature, altitude, and physiological factors such as age, physical fitness, nutrition among several others (Zakynthinaki, 2015). For exercise of constant sub-maximal intensity the HR remains at a constant rate which is obtained after a certain time. However, for higher intensity levels the HR may never reach a steady state and rather experience a slower increase after some time (Zakynthinaki, 2015).

In previous parts of the DigiW project the stages of the experiments have been looked at in isolation and attempted to be fit with linear first order models. The conclusion from these were that a first order model was not sufficient in explaining the kinetics of the HR and that an integrator should be included in the model to achieve better fit (Cappozzo, 2022). Therefore, development of a dynamical model to capture the dynamics of HR during PA have been investigated in the following thesis.

2.1.2 IPAQ

International Physical Activity Questionnaire (IPAQ) is a questionnaire developed for evaluation of physical activity (PA) in adults in the age range 15-69 years. IPAQ is a self-report survey where the participant reports minutes of physical activity within an average week. Activity is categorized into three intensity-levels: walking, moderate and vigorous. The participant separates active minutes throughout their week into each respective category. All domains of activity count towards the reported time, for instance domestic, work- and transport-related activities within the same intensity level will contribute equally to the total. The intensity levels however, are weighted by their energy requirements in terms of METS, which are multiples of the resting metabolic rate and when multiplied by duration of activity in minutes result in a score given in MET-minutes. A value in MET-minutes may be converted to kilocalories through the following formula:

$$kcal = MET - min (weight [kg] / 60 [kg]) \quad (1)$$

The values used for MET in this thesis are shown in table 3 and have been derived from the IPAQ reliability study (IPAQ, 2004).

The total MET score, reported as a median for each participant is thereby calculated by equation 2, where the number of minutes performed at each level; walking (W), moderate PA (M) and vigorous PA (V), is multiplied by the number of days the participant performs the amount of

minutes at the given level per week.

$$MET_{total} = 3.3 \min_W \text{ days}_W + 4.0 \min_M \text{ days}_M + 8.0 \min_V \text{ days}_V \quad (2)$$

It should be noted that only bouts of duration longer than 10 minutes are recorded in the survey, as this is the required length for receiving health benefits from the effort (IPAQ, 2004).

2.2 System identification

System identification is the use of data to develop models for a given system. The model is then a simplified version of the actual system, in order to be a viable model it should adequately mimic the essential features of the data. Models consist of two parts: structure and parameters. The model-structures considered in this thesis are presented below. Numerical optimisation, as presented in Section 2.3 was used as a method of estimating the parameters.

2.2.1 First order model

A linear, time-invariant and driven first order model is given in the following equation (Andresen et al., 2016):

$$\dot{x}(t) = f(x, u, t) = \alpha x(t) + \beta u(t) \quad (3)$$

Relating this to the physiological case regarded in this thesis, it may be translated to the following:

$$\dot{HR}(t) = \alpha HR(t) + \beta u(t) \quad (4)$$

Thereby, the derivative of the heart rate, is related to the heart rate and an input, u , by the constant parameters α and β . In the discrete case a general first order model can be formulated as in equation 5 where k is a discrete time-step.

$$x[k+1] = \alpha x[k] + \beta u[k] \quad (5)$$

The above functions are examples of linear models, however, by making one of the terms nonlinear, for example by squaring or adding a geometric term, the model becomes nonlinear.

2.2.2 Second order model

A second order model includes the 2nd order derivative in the description of the system, such models can always be written as a set of first order equations as is done when rearranging equation 6 into the set given in equations 7 and 8.

$$\ddot{x}(t) = f(\dot{x}, x, u, t) = \alpha_1 \dot{x}(t) + \alpha_2 x(t) + \beta u(t) \quad (6)$$

$$\dot{x}_1(t) = x_2 \quad (7)$$

$$\dot{x}_2(t) = \alpha_1 x_1(t) + \alpha_2 x_2(t) + \beta u(t) \quad (8)$$

This is again a linear, driven model. In general, second order models may have more intricate functions and relations than shown here. The set of equations can be discretized by the same method as was done for the first order system.

2.3 Numerical optimization

Numerical optimization methods are used to minimize or maximize some objective-function, all these methods can be generalised as trying to find the variables, x , that satisfy the following equation

$$x : \min_{x \in R^n} f(x) \quad \text{s.t.} \quad \begin{aligned} c_i(x) &= 0, \quad i \in \varepsilon \\ c_i(x) &> 0, \quad i \in I \end{aligned} \quad (9)$$

Gradient-based optimization methods update the variables step-wise along the gradient of the objective function until a solution that satisfies the requirements is found. Such methods often use many iterations to converge, hence the development of Newton methods. Newton methods consider not only the gradient, but also the Hessian when making updates, this causes the algorithm to take better steps towards the minimum and thus converges in fewer iterations. A more complex group of optimization methods are the quasi-Newton methods. These methods are less computationally expensive variants of the aforementioned Newton-methods, which consider the Hessian of the objective function. The quasi-Newton methods use an approximation of the Hessian instead (Nocedal and Wright, 2006). As a general rule these methods makes the variable update, x_k to x_{k+1} , according to the formula described in equation 10, where α_k is a step-length that satisfies the Wolfe-conditions and B_k is a non-singular approximation of the Hessian (Hauser, 2005).

$$x_{k+1} = x_k + \alpha_k(-B_k^{-1}\nabla f(x_k)) \quad (10)$$

The function $f(x)$ however must be twice differentiable and convex.

2.3.1 Broyden–Fletcher–Goldfarb–Shanno algorithm

One of the quasi-Newton methods is the Broyden–Fletcher–Goldfarb–Shanno (BFGS) method, in which B_k is not recomputed at every iteration, but rather updated by accounting for the curvature in the previous iteration (Nocedal and Wright, 2006). Following the derivation given in Nocedal and Wright, 2006 on page 137, B_k can be found through equation 11.

$$B_{k+1} = B_k - \frac{B_k s_k s_k^T B_k}{s_k^T B_k s_k} + \frac{y_k y_k^T}{y_k^T s_k} \quad (11)$$

The initial B_0 can be set as an approximation of the Hessian or another arbitrary matrix, such as the identity, or a scale-reflecting multiple of it (Nocedal and Wright, 2006). The method known as Limited Memory BFGS-B is commonly used in programming cases with bounds on the variables (Zhu et al., 1997).

2.4 Least squares estimation

Least squares is a widely used estimator for parameter identification. It attempts to identify the most probable values for the parameters, which is defined as the value that makes the residuals as small as possible (Sorenson, 1970). Mathematically, it can be formulated through equation 12, where x_i are the points in the actual dataset, $f(x, \theta)$ is the function which characteristics are defined by the parameters θ .

$$\hat{\theta}_{LS} = \underset{\theta}{\operatorname{argmin}} \sum_{i=1}^n (y_i - \hat{f}(x_i; \theta))^2 \quad (12)$$

where i is the number of data points.

2.5 Measurements of performance

2.5.1 Coefficient of determination: R^2

R^2 , defined as coefficient of determination, is a measure of goodness-of-fit of a model to a dataset. It is based on the mean squared error (MSE) of the model. The MSE is the square of the residuals, that is the distance between the actual data points and the points predicted by the model. Its formula is given in equation 13, where n is the number of data points, y_i , \hat{y}_i are the models' predictions and \bar{y} is the average of the datapoints. Thus, R^2 is given by formula 14.

$$MSE = \frac{1}{n} \sum_{i=1}^n (y_i - \hat{y}_i)^2 \quad (13)$$

$$R^2 = 1 - \frac{\sum_{i=1}^n (y_i - \hat{y})^2}{\sum_{i=1}^n (y_i - \bar{y})^2} \quad (14)$$

A high R^2 indicates a good fit, the lower the value is the worse is the model in explaining the variance in the data. An R^2 close to or below 0 shows little to no statistical significance. When working with behavioural data however it is common to accept a much lower value than most other cases due to human errors (Walpole et al., 2016).

FIT is another way of presenting the coefficient of determination. Essentially, the metric is the same as R^2 , but given as a percentage and the higher it is the better is the fit, it may have a negative number.

2.6 Fourier transform

The Fourier transform transforms a signal in the regular time-domain into the frequency-domain. The magnitude at each frequency represents the presence of that frequency in the original signal. One may change the original signal by removing certain frequencies in the transformed signal. A signal expressed as a function of frequencies, s is denoted as $\hat{f}(s)$ may be defined through the Fourier transform given in equation 15 where i is the imaginary unit (Osgood, 2007, p. 76).

$$\hat{f}(s) = \int_{-\infty}^{\infty} e^{-2\pi i s t} f(t) dt \quad (15)$$

For the purpose of this thesis this transform may be useful to remove the higher order frequencies as a method for removing rapidly fluctuating noise in the signal.

2.7 Correlation analysis

Correlation coefficients are measures of the degree of linear association between two variables (Walpole et al., 2016, p. 451). Essentially the correlation between variables is their covariance, standardized by their standard deviations. The Pearson correlation coefficient between variables x and y is given in equation 16.

$$r = \frac{S_{xy}}{\sqrt{S_{xx}S_{yy}}} \quad (16)$$

In which S_{xy} , S_{xx} and S_{yy} each are measures of the variability of each variable, defined as shown below, with \bar{x} and \bar{y} being the average of the two variables, (Walpole et al., 2016)

$$\begin{aligned} S_{xx} &= \sum_{i=1}^n (x_i - \bar{x})^2 \\ S_{yy} &= \sum_{i=1}^n (y_i - \bar{y})^2 \\ S_{xy} &= \sum_{i=1}^n (x_i - \bar{x})(y_i - \bar{y}) \end{aligned}$$

When the correlation-coefficient is positive it means that there is a linear relationship between the variables, where an increase in one corresponds to an increase in the other. Negative correlations are the opposite, where an increase in one variable corresponds to a decrease in the other. Correlation-coefficients are in the range -1 to 1, where each of the extremes represent fully negative- and positive correlations respectively.

3 Method

3.1 Pre-processing and Data cleaning

This thesis was based on data collected through different sensor and devices in the DigiW-project, as explained in the section 1.2.3. More specifically the analysis in this thesis used the continuous HR signals from the experiments, in combination with demographic information about each participant. Thereby, the thesis was based on several timeseries-data over periods upwards of 2 hours. In order for the data to be useful, quite a bit of pre-processing and data cleaning was needed. A significant part of the project was spent handling this aspect. Several different methods for structuring and imputing the data were attempted in order to create a pre-processing pipeline for all participants that conserved all biological properties of the data.

The data-collection process in itself was standardized for all participants. However, there are always challenges with adhering to a standardized protocol when it comes to experiments performed by human individuals. Figures 3 and 4 show the raw HR signals from one participant over two full experiment days. The plot shows some of the variances that may occur during the experiment. The most apparent divergence from standard procedure here is the rest-length between periods, which is seen in figure 3 where the rest between the first and second stage is significantly longer than that between the second and third. Figure 4 shows a participant unable to complete the last stage and therefore terminating it early, this is another case of the general experiment-design which is often diverged from. These are the two most common cases needed to account for in the processing and the analysis of the data. This experiment in particular is incredibly vulnerable to human efforts affecting the data since the participant are asked to physically exert themselves and certain tasks have to be performed in a physically exerted state.

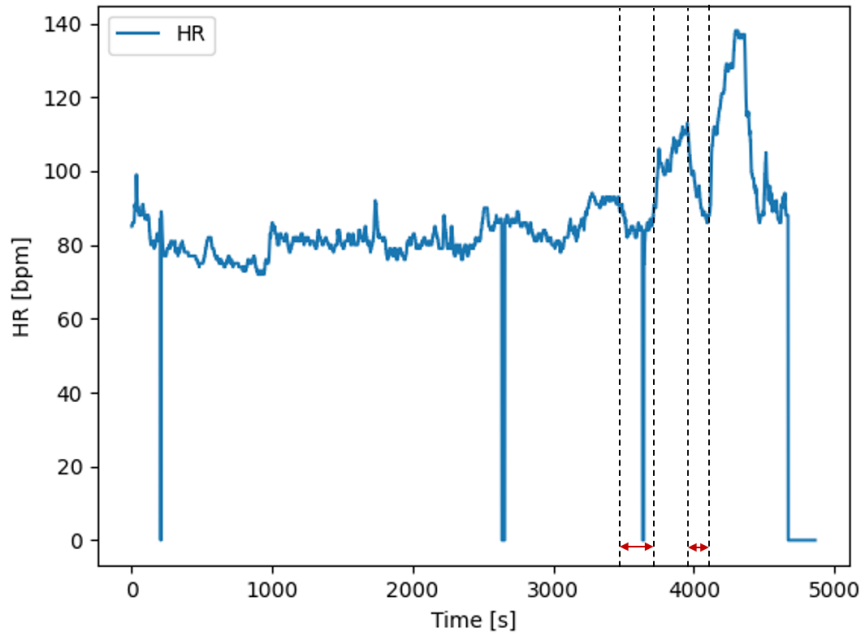


Figure 3: Raw HR signal from one experiment day from polar sensor located around a participant’s chest with annotations indicating rest-periods

The experiments were performed as part of a large interdisciplinary study which is the reason for the large amount of different sensors and data collected in the experiment. This lead to some of the issues with divergences from the standardized time-intervals as large amounts of sensors heightens the need for prolonged rest in order to fix a sensor. However, the main challenge with this accumulation of sensors was that their data needed to be synchronized. No standardized and synchronized timestamps existed to indicate when stages started and stopped for all participants and these varied greatly due to human variances in the experiments, as was displayed in figures 3 and 4. Therefore start- and stop-times had to be interpreted from the recorded signals and

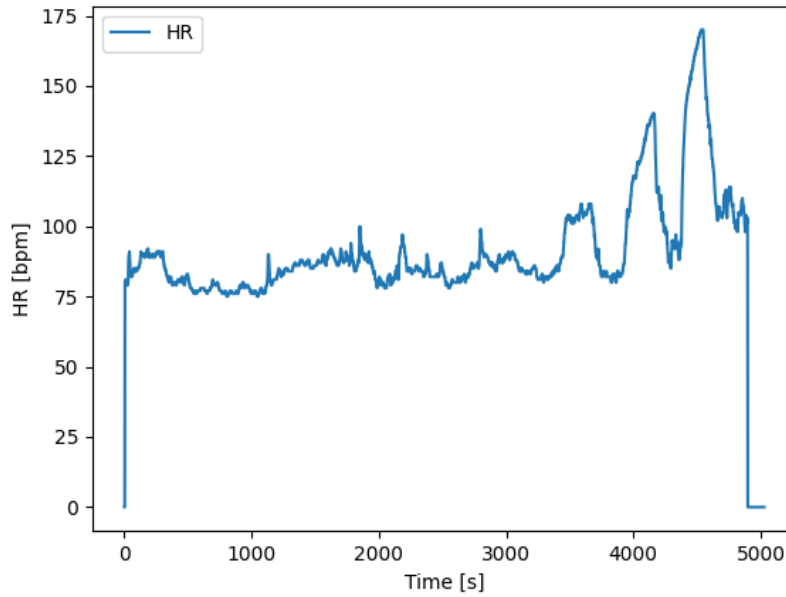


Figure 4: Raw continuous HR signal from polar sensor located on the participant's chest.

the manually recorded timestamps per day. For the purpose of this thesis, the HR data needed synchronization to an input-signal which was done through synchronizing with the aforementioned manually recorded timestamps.

Another result of the multiple uses of the data was that the data recorded over a longer timeframe than needed for the scope of this thesis. Before the interval stages, and after some of them, there are long periods of recorded data that we did not want to include in the following analysis. These sections of the timeseries were used to determine a median of the HR to represent the resting HR. After using these sections for that purpose, everything up until the end of the warm-up was removed, as well as everything after 120 seconds after the last stage.

3.1.1 Missing data

The HR data used in this thesis stemmed from a Polar HR sensor, detailed in Section 1.2.3. The participant had this mounted around their chest throughout the entire duration of each day, for consistency of measurements. However, there were still some challenges with the signal obtained from the HR sensor, that required handling in pre-processing of the data.

The main issue was the general noisiness of the HR signal. This was a result of the underlying challenges of this type of measurement. Measurements of physiological factors through skin, and tissue tends to be erroneous as several varying factors between individuals affect the measurements. Movement and sweat which may vary throughout the experiment impact the sensor and create noise. This makes it hard to interpret the signal and correctly determine true value. Examples of the raw signals are shown in figures 3 and 4. The noise is particularly apparent before the warm-up where the participant is at rest. Ideally, the HR-signal should be constant and representative of the resting-HR within this time frame. As can be seen from the figures, the HR oscillates within a range of about 10 bpm and has additional large erroneous spikes. This had to be carefully considered whenever making choices on how to deal with this data.

The HR monitor had a tendency to fall-out during the experiment meaning that it had periods where it did not record any measurements. This happened in single sample instances, examples of which is displayed as zero-values in figures 4, but there were also minute-long periods where the HR monitor did not collect measurements, as displayed in figure 5. Initially the missing values were simply imputed with the next valid value, which worked well for the cases where individual samples were missing. However, when there were periods lasting several minutes without any

recorded data, this method potentially altered the signal greatly in a wrong direction, due to the added issue of noisiness in the data. The resulting method used for imputation of these values was then to impute the missing values with the mode of the remaining signal. The mode was chosen as the imputation value, instead of the mean as this is a more accurate representation of the resting HR, due to the fact that the participants were in activity for large portions of the recorded signal.

The sensors were particularly susceptible to missing values when the participant transitioned between different sections of the experiment. The transition between the rest periods and activity on the treadmill was the most crucial as this might be included in the partition of the signal we wished to use. There were also vulnerable periods at the beginning and end of the experiment days, but these were simply disregarded.

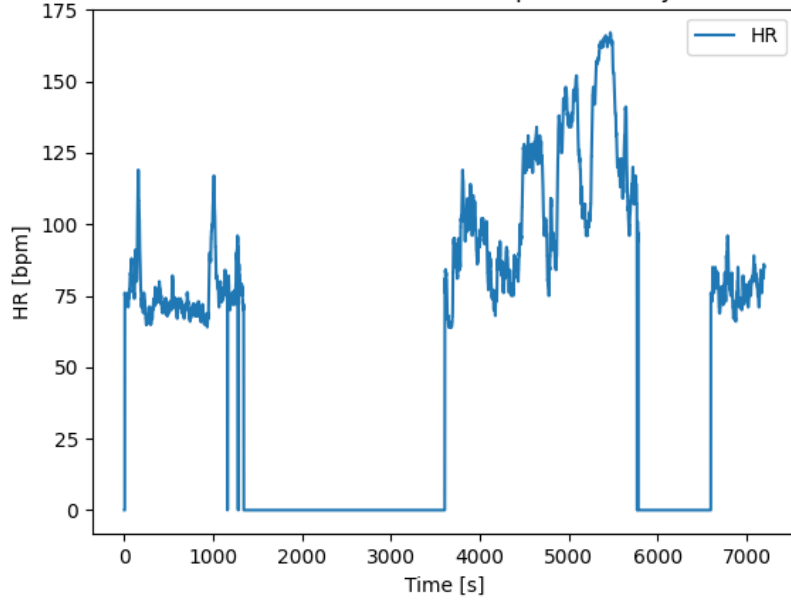


Figure 5: Raw HR signal from one full experiment day for one participant displaying long periods of missing records.

3.1.2 Smoothing

Due to the high variability in the HR-signal, which was seen previously to oscillate rapidly even in steady state. An attempt was made to smooth the signal, in hope that it could produce better fits of the model. This smoothing was performed using a Fourier transform, as described in the theory. After the Fourier transform, the higher frequencies were removed from the signal in order to capture the bigger tendencies of the signal. Figure 6 shows the resulting smoothed signal by use of a Fourier transform. The issue with this, is that the dynamics of the HR is indeed quite rapid by nature and thus in removing the noise, we also removed some of the naturally fast dynamics of the HR. A trade-off had to be made between the two.

3.1.3 Input construction

The aim was to find a model that predicts the HR based on an input, thereby a signal for the input had to be constructed. The generation of the input signal was based on manually recorded values of the start- and stop-times of each stage. The inputs were generated in two variants which both try to emulate intensity, one where the input is simulated as a combination of the speed and incline of the treadmill and one where these are given as two different parameters. This is shown in Figure 7 and 8 respectively. Both input-types were used in the system identification. We aimed to see which one could better explain the dynamics of the data and give a better model fit and also see what the model can tell us about the importance of the two factors in prediction of HR.

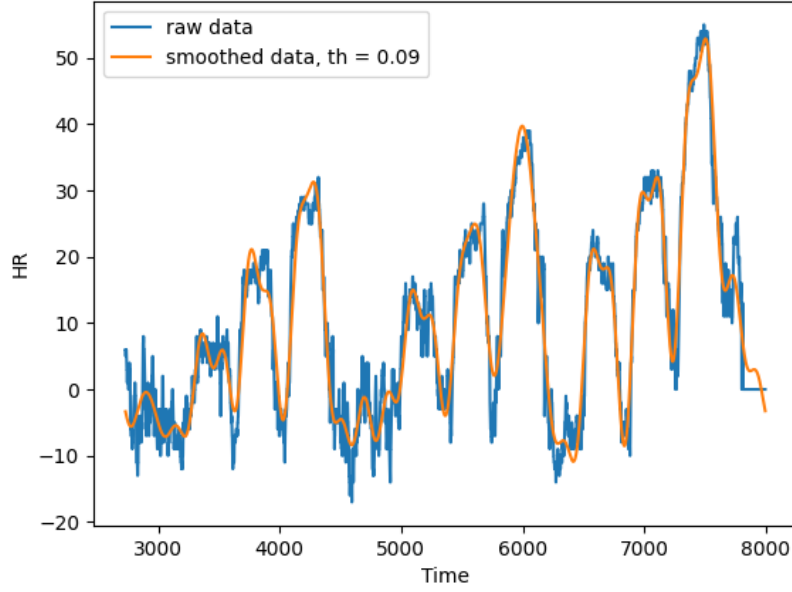


Figure 6: Raw HR data and data smoothed with Fourier transform. Data stems from one full experiment day for one participant. 'th' is the threshold used to determine which frequencies to remove from the signal

3.2 System identification

3.2.1 Data organization

As described in the test protocol in the introduction, each participant conducted a total of 9 stages distributed over three test days, where each day was dedicated to a set incline on the treadmill. As these stages, and the rest-periods between them were the targets of the analysis in this thesis, everything else was removed from the raw data. The separate days were concatenated to form one continuous signal to use in the system identification process. The previous attempts at trying to find models and model-parameters, have looked at one stage in isolation, the goal here was to see if one set of parameters could work well to represent all stages and days simultaneously. Thereby, every time an individual is active due to a known input it will show a response defined by a fixed set of parameters. So, it should be possible to individually decide a set of parameters, for which the persons HR always will follow based on input. The resulting dataset that was used in analysis takes on the general shape that is shown in figure 9, which shows the specific case for one participant.

As specified before, the mode of the measurements was removed from each experiment-day. This was done as a regularization-measure so that the resting-HR of each participant, which may be regarded as an offset, does not impact the resulting parameters from the identification. Consequently, what is from now on labeled as HR in the plots is actually the HR but subtracted its mode. This explains why the HR seems to be below biologically viable values.

From figure 9 one can clearly see the nine stages as the impulses with heightened HR. The first three correspond to the first test day with incline 0.5 %, the next three impulses stem from the second day with incline at 2.5%, note that the incremental stage at the end of this test day has been removed, the last three pulses are from the third day with incline 5.0%. Speeds of each stage on each day can be found in table 2. It should be noted that even though participants performed the respective days in a randomized order, for simplicity they have all been concatenated in the order given above, irrespective of the order they were performed by the participant.

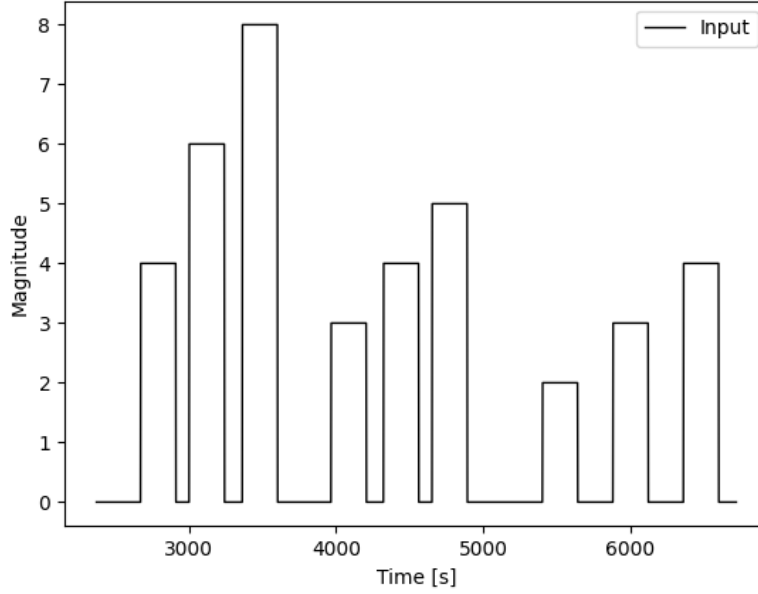


Figure 7: Input signal constructed as a single source based on a combination of speed and incline of the treadmill. The y-axis gives the magnitude of the input and has no direct physical interpretation in terms of units.

3.2.2 Cost function

We applied system identification methods to identify the parameters of the potential model structure. The parameters were found by employing numerical optimization on a cost-function. A least-squares estimation approach was selected. The motivation behind this identification was that we think every participant has a set response to input. Thereby, the cost-function we seek to minimize is defined by equation 17 where the indexes 1, 2 and 3 correspond to the three test days. The cost of each test day is given by the summed square of residuals as show in equation 18

$$Cost = \sum_{j=1}^3 cost_j \quad (17)$$

$$cost_j = \sum_{i=1}^n (y_i - \hat{y}_i)^2 \quad (18)$$

3.3 Numerical optimization

Numerical optimization, more specifically L-BFGS-B method was used to find a minimum in the cost function given above. The cost function was a least squares measure of a model with a set of parameter's fit to the data. Thus the algorithm seeked to find the parameters which minimizes the sum of squares between the data points and the points predicted with the set parameters based on the specific model. The optimization was bounded in the sense that we need the parameters to be in the range $[0, 1]$ in order to ensure stability in the discretized system (Andresen et al., 2016, p.531).

From hereon, to simplify notation, the HR will be denoted as x , the constructed single-input as simply u and incline and speed as u_1 and u_2 respectively. When the input is denoted as a vector \mathbf{u} it is to signify that both the single input and the separated has been used in that setting.

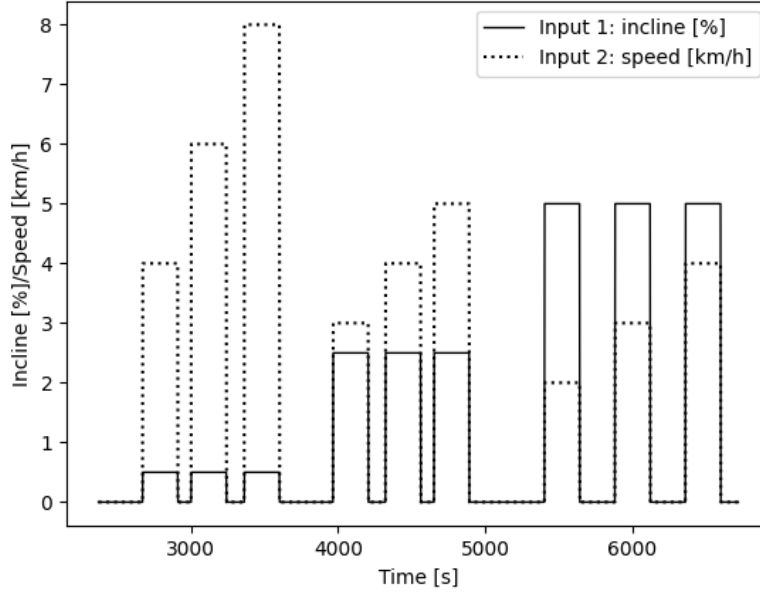


Figure 8: Input signal constructed as two separate sources, one is the speed [km/h] and the other is the incline [%] of the treadmill

3.4 Model structures

Several different model structures were implemented and fit to the data as in the process explained above. The following subchapters provide the discretized formulas for each of the implemented model structures.

3.4.1 First order linear model

As described in the theory, with the start of the PA, HR will increase from resting state and reach a constant value thereafter, this concept is visualised by the HR signal from one participant over one stage in figure 10. A first order linear model defined in the following is selected as a candidate structure.

$$x[k+1] = \alpha[k] + \beta \mathbf{u}[k] \quad (19)$$

$$x[k+1] = \alpha[k] + \beta_1 u_1[k] + \beta_2 u_2[k] \quad (20)$$

where $x[k]$ is the HR at timestep k , and α and β are the target parameters to be identified by minimizing the cost-function described in 17. The input \mathbf{u} was implemented either as the constructed single source input or the speed and incline as separate inputs, u_1 and u_2 , in the second case both β_1 and β_2 are identified.

3.4.2 First order nonlinear models

Several first order nonlinear model structures were also investigated. The main focus was at attempting to square the input. In the case with the input modelled as a single source, it was squared as in equation 21

$$x[k+1] = \alpha[k] + \beta u[k]^2 \quad (21)$$

In the cases where the input is separated into incline (u_1) and speed (u_2), the model given in 22 was implemented.

$$x[k+1] = \alpha[k] + \beta u_1[k] u_2[k]^2 \quad (22)$$

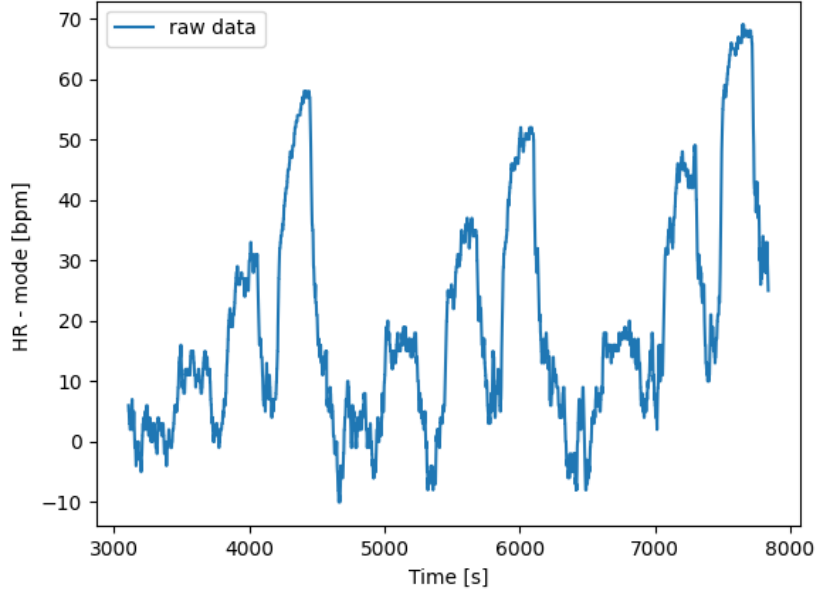


Figure 9: Concatenated HR of all test days for a single participant. Missing signals were imputed with the mode, and the mode has been subtracted from all points.

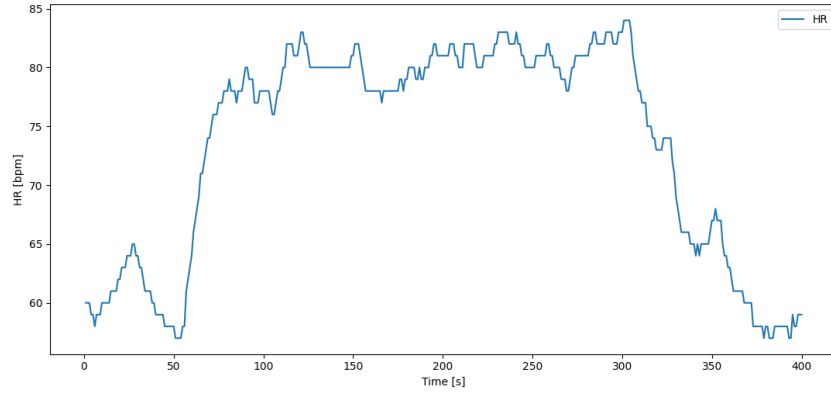


Figure 10: HR-signal from one stage for one participant showing similar response to a first order system

3.4.3 Second order linear model

As an attempt to include the slower cardiac increase that was explained in the theory and is visualised in figure 11, second order models were fit to the data. These were implemented as described by the following equations.

$$x_1[k+1] = \alpha_1 x_1[k] + x_2[k] \quad (23)$$

$$x_2[k+1] = \alpha_2 x_2[k] + \beta \mathbf{u}[k] \quad (24)$$

3.4.4 Second order nonlinear models

For the second order models, the nonlinear model structures given below were implemented, where u_1 is the incline and u_2 is the speed.

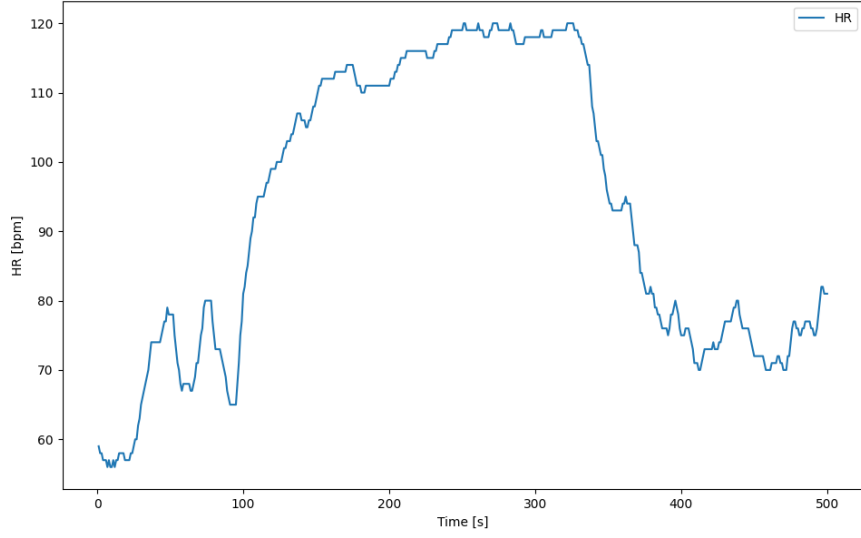


Figure 11: HR-signal from one stage for one participant showing similar response to a second order system with integrating effect

$$x_1[k + 1] = \alpha_1 x_1[k] + x_2[k] \quad (25)$$

$$x_2[k + 1] = \alpha_2 x_2[k] + \beta \mathbf{u}[k]^2 \quad (26)$$

$$x_1[k + 1] = \alpha_1 x_1[k] + x_2[k] \quad (27)$$

$$x_2[k + 1] = \alpha_2 x_2[k] + \beta u_1[k] u_2[k]^2 \quad (28)$$

4 Results

In this section results with regards to simulating different model structures, identification and correlations among parameters and participants' personal characteristics are reported.

4.1 First order linear model

Data collected from one specific participant is used to visualize the performance of different model structures in tracking HR dynamics. The participant was chosen based on goodness of HR-data.

Figure 12 shows the result of the first order model identification given by equation 3 where the input was modeled as a single source. The simulation in figure 12a was performed with the parameters estimated from the raw HR data. The simulation in figure 12b is the output from the simulation with the raw HR-data as input, but the parameters used in the simulation were found through minimization of the cost-function with a smoothed version of the HR-signal. The difference between the two versions is that 12b has longer time-constants. Both of the models grossly over-estimate on all stages of the first experiment day, and underestimate by a similar amount on the three stages of the third day.

The average of each estimated parameter, the average fit and the standard deviation of each of these are given in table 4 and 5.

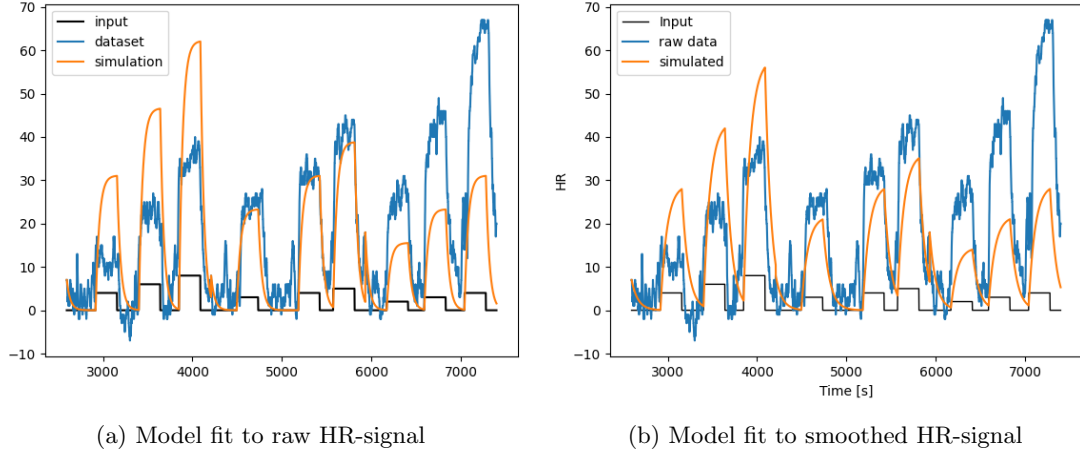


Figure 12: First order linear model fit to one participant for an entire experiment day

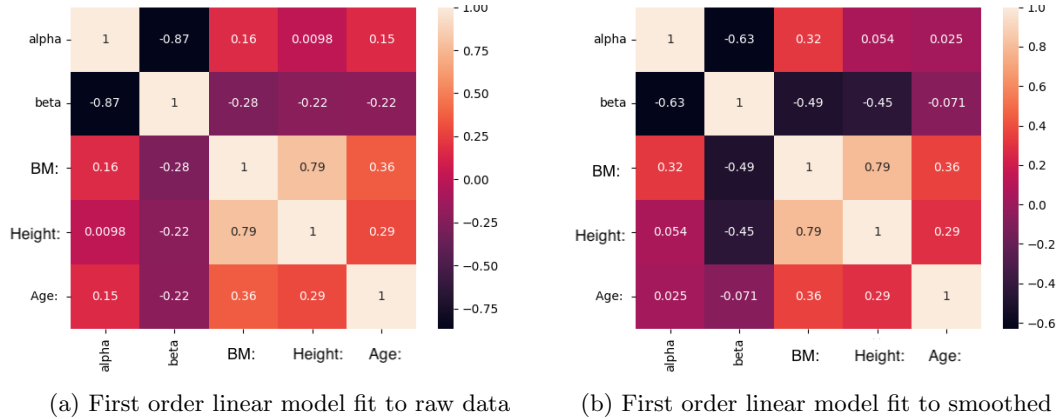


Figure 13: Heatmap of correlations between demographic variables and parameters obtained for the first order linear models

Correlation coefficients were calculated, as by formula given in the theory, and displayed in correla-

tion heatmaps. Figure 13 shows a heatmap of the correlation-coefficients between the demographic variables and the parameters obtained by the first order linear model identification. IPAQ and gender are not included here as they are categorical values. The parameters correlate with themselves to a large extent as can be seen by their high absolute values, and so does certain of the demographic variables with each other, such as weight and height. The strongest correlations between demographic variables and parameters are found in the model derived from the smoothed data. β has correlation-coefficients of -0.49 and -0.45 with weight and height respectively as seen in figure 13b.

Each participant has a numerical IPAQ-score and a categorical IPAQ-score. The MWU only have categorical scores, and are all within the same category, therefore correlations with IPAQ have only been calculated for AB. The correlation-coefficient between the parameters and IPAQ-score can be found in table 6, which shows a nonsignificant correlation between the two for this model.

Figure 14 shows the simulated response for a linear first order model where the input was given as the speed and incline separately. Compared to when the input was a single value the model follows the raw data more closely. Although some overestimation for the first day and underestimation of the last day still persists, this offset is reduced. The performance is reflected in the fit statistics presented in table 4 and 5. When comparing the model generated from the smoothed signals to that based on the raw there is a much larger difference here than in the previous case. The smoothed data yields a higher α indicating a longer time constant. The parameters and fit are similar for AB- and MWU-group. The heatmaps 15a and 15b show the correlation-coefficients

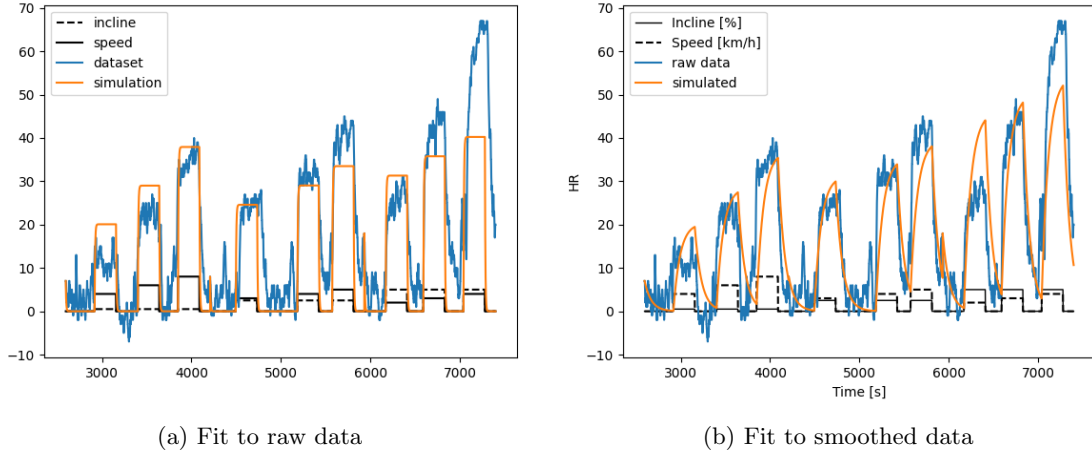


Figure 14: First order linear models based on separated input, fit to one participant over all experiment days

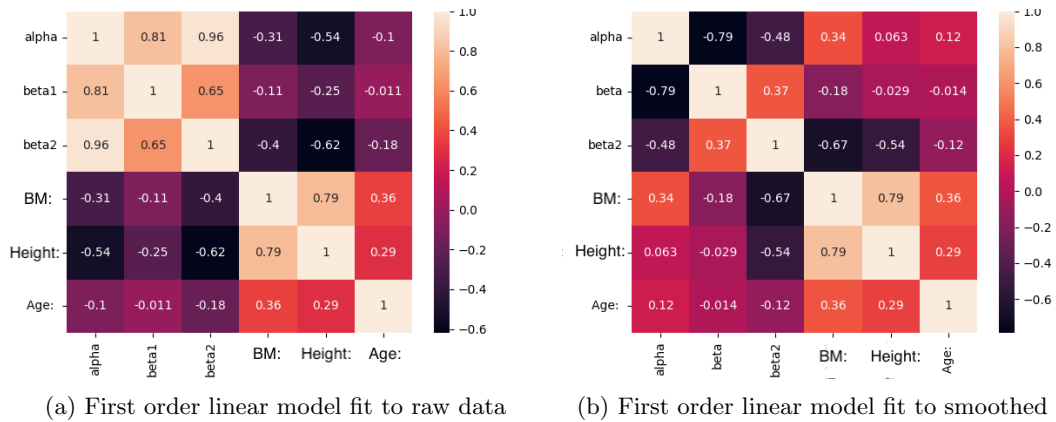


Figure 15: Heatmap of correlations between demographic variables and parameters obtained for the first order linear models with separated input

for this model. Generally there are higher coefficients here than in the previous model, indicating better correlations. Again, the height and weight stand out as the parameters with the highest coefficients. In this case they have non-insignificant correlations with α - and both the β -parameters.

In order to see if the parameters could be used to individualize the HR predictions, correlation analysis has been employed and results has been shown in three dimensional plots. These plots were separated by gender and parameters were plotted against age, height and body-mass to find any potential correlations. Figure 16 shows the parameters obtained from this system identification plotted against different demographic variables for each of the participants; gender, age, body-mass and height. Supporting what was seen in the heatmap in figure 15a some correlation can be detected between the height and the obtained parameters in 16c and 16e.

4.1.1 First order nonlinear model

The nonlinear model based on a single input was implemented as shown in equation 21, the simulation results can be found in figure 17. This model shows the same over- and underestimation tendencies that were prevalent in the first order linear model. And in this model where the input was squared this tendency was enhanced further and yields an even lower fit, regardless of whether the model was optimized on the raw or smoothed data. This is shown in table 4 and 5. The parameters for AB and MWU are similar and yield equally low fit. Figure 18 shows that there are no significant correlations from this model.

The model implemented as in equation 22 yields the performance shown in figures 19a and 19b. The parameters and fit statistics are presented in table 4 and 5, these are similar to what was obtained in the first order linear model with separated input. From the raw data there are no significant correlations seen in figure 20a, however the results from the smoothed data in 20b show correlations between the parameters and the participant's weight and height. Table 6 shows that here is a small negative correlation between the IPAQ and the α -parameter.

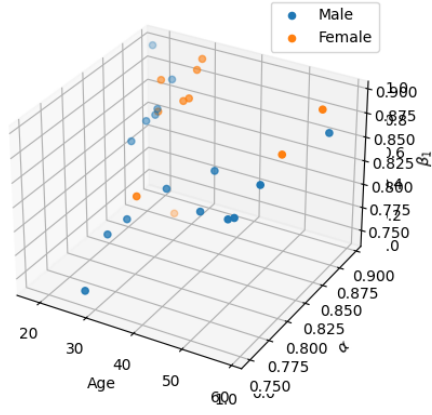
Figure 21 shows the corresponding three-dimensional plot of the nonlinear first order model. These plots supports the correlations seen in the heatmap, and moreover exposes gendered groupings which gives rise to possibilities of splitting the parameters into gendered ranges. As can be seen from 21c and 21b especially, the female participants generally have higher β than the male participants.

4.1.2 Second order linear model

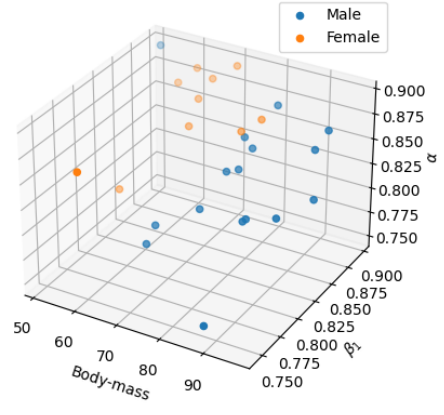
The second order model was implemented as described in equation 6. Figure 22 shows the simulations obtained with these models, table 4 and 5 shows the corresponding parameters and fit statistics. Figure 22b shows the same tendencies as in the first order linear model with the same single input source, where there was overestimation on the first day and underestimation on the last. Tables 4 and 5 reiterates that the fit of this model is the lowest obtained so far.

Similarly to the first order model, the fit was significantly increased when speed and incline are used as separate inputs. The performance is shown in figure 24 and the fit statistics are presented in table 4 and 5. The dynamics of the model obtained from the raw signals are, as shown in figure 24, much faster than the dynamics stemming from the smoothed signal, which can be seen in figure 24b.

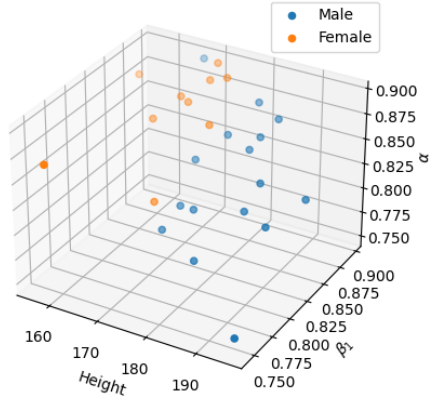
Figure 26 shows the parameters plotted against the demographic properties. The parameters from the smoothed model were used since these had the best fit to the data as can be seen by the difference in 5 and 4. What is apparent from these plots is that the α s are high for all participants, except two outliers and the β s are small for all except the same two outliers. No correlations are found between the variables and there are no apparent groupings either.



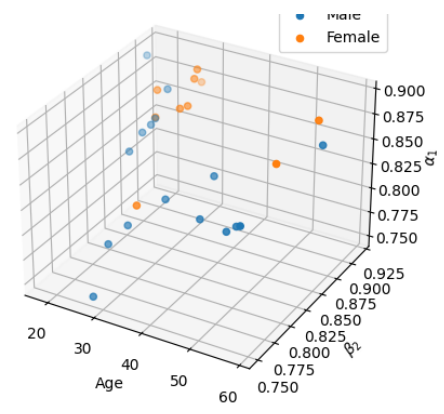
(a) Age vs. α vs. β_1



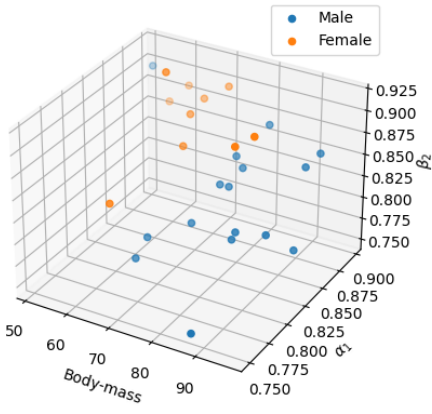
(b) Body-mass vs. α vs. β_1



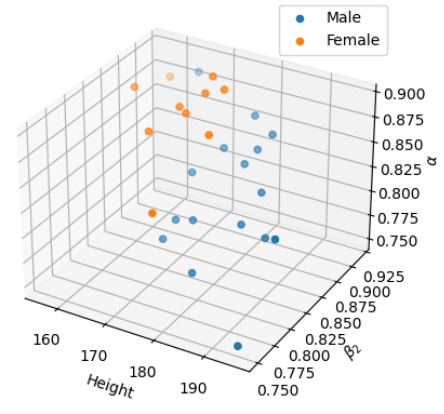
(c) Height vs α vs. β_1



(d) Age vs. α vs. β_2



(e) Body-mass vs. α vs. β_2



(f) Height vs α vs. β_2

Figure 16: Parameters obtained from the first order linear model, with separated input when fit to the smoothed data, plotted against characteristics of each participant

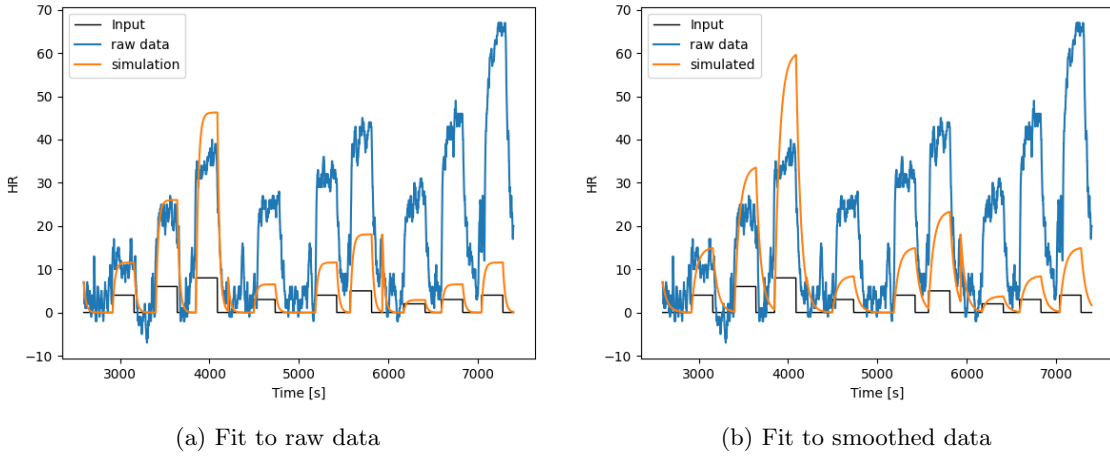


Figure 17: First order nonlinear model, with single input fit to a participant over all days

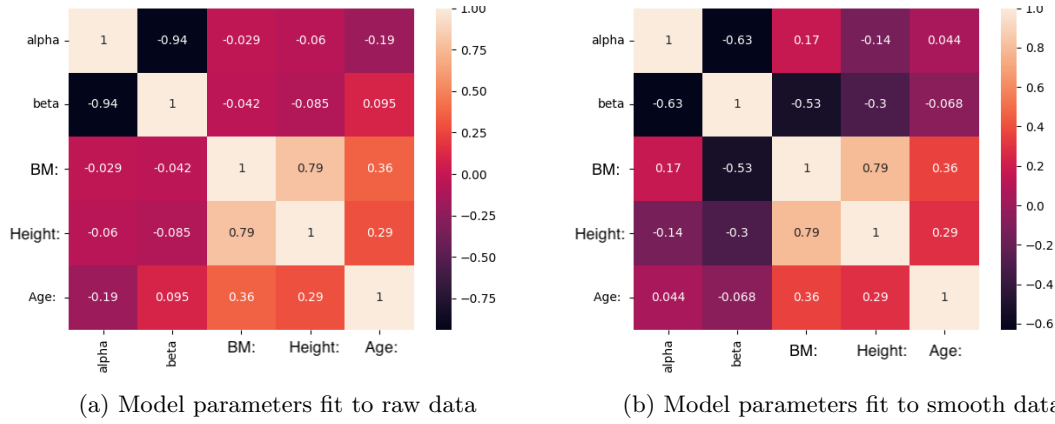


Figure 18: Heatmap of correlations between demographic variables and parameters obtained from the first order nonlinear model with single input

4.1.3 Second order nonlinear model

The results from the implementation given in 7 are shown in figure 27 and parameters and fit statistics are found in table 4 and 5. Once again the model with single input has an inadequate performance and in this case shows consistent underestimation. The correlations for this model found in figures 28 are not representative due to the low fit of the model.

The results from implementation of a second order nonlinear model with separated input, as given in equation 8 are shown in figure 29 and the tables 4 and 5. The fit achieved here is similar to that achieved by the first order nonlinear with separated input as described earlier. The parameters obtained from the model based on smoothed data, show moderate correlations between the weight and all the parameters, these are given in Figure 30 and table 6. The three dimensional plots of parameters in Figure 31 show no apparent gendered groupings.

4.2 Model summary

Comparing all the attempted models, it is clear that the models that achieve the highest fit in both the first and second order are the nonlinear models with separated input. Figure 32 shows the two plotted together for comparison.

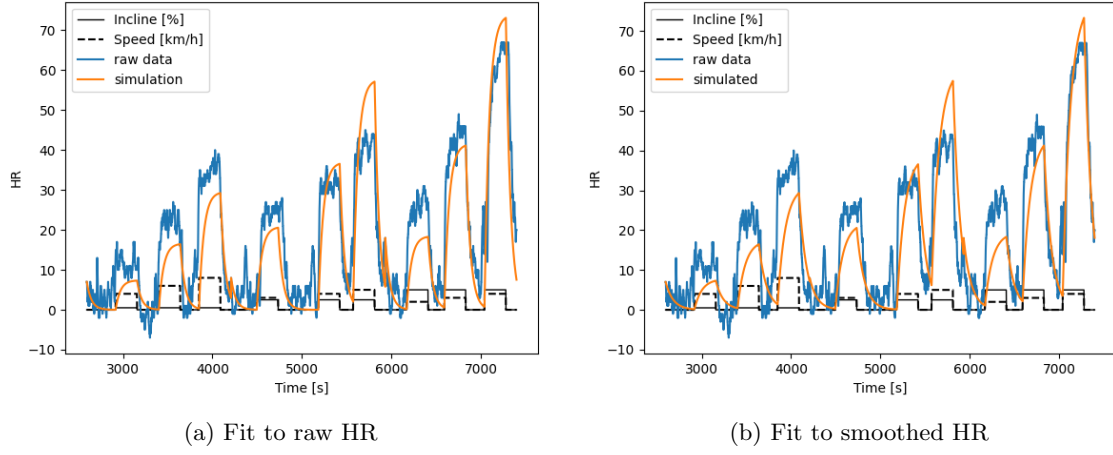


Figure 19: First order nonlinear model, with the input separated into two, fit to one participant over all experiment days

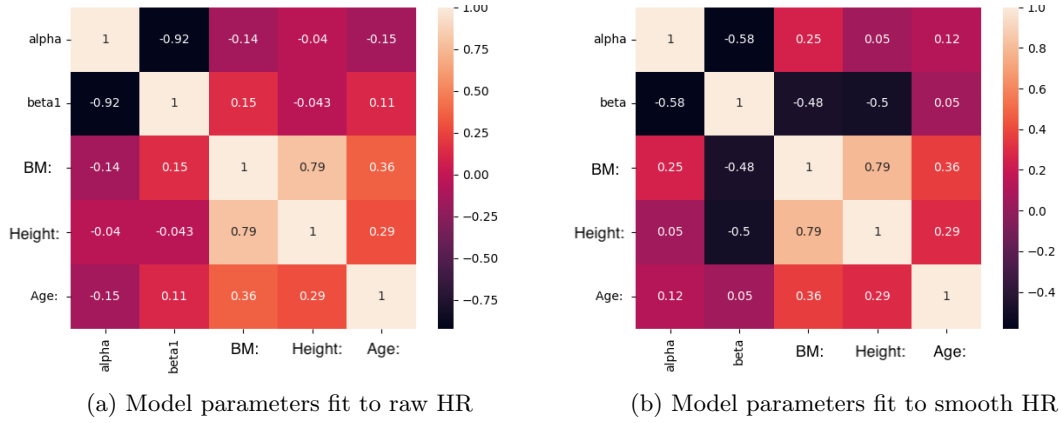


Figure 20: Heatmap of correlations between demographic variables and parameters obtained from the first order nonlinear model with separated input

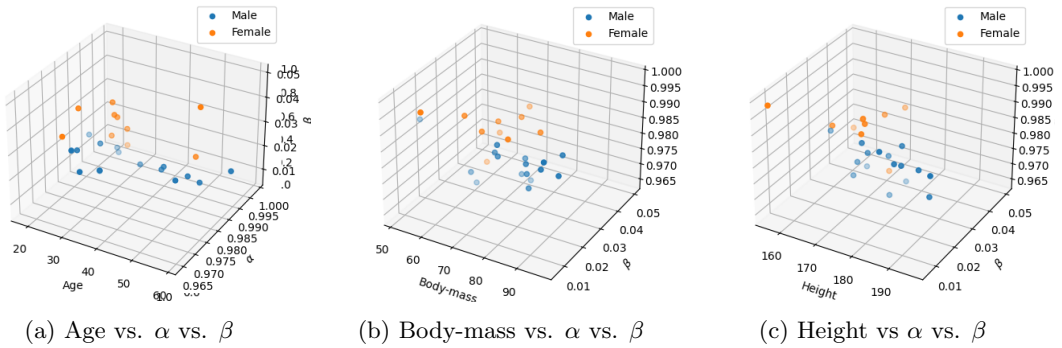
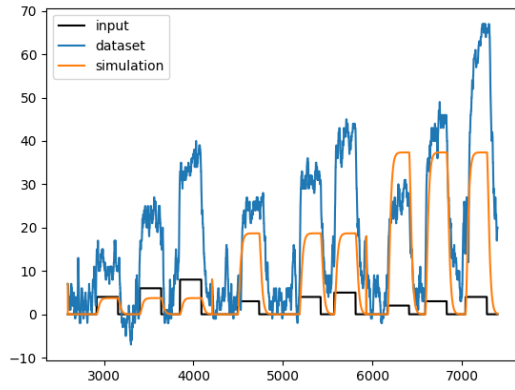
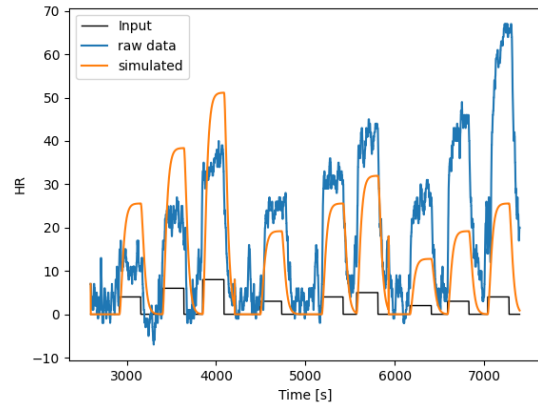


Figure 21: Parameters of the first order nonlinear model with separated input based on the smoothed data, plotted against physical properties of each participant

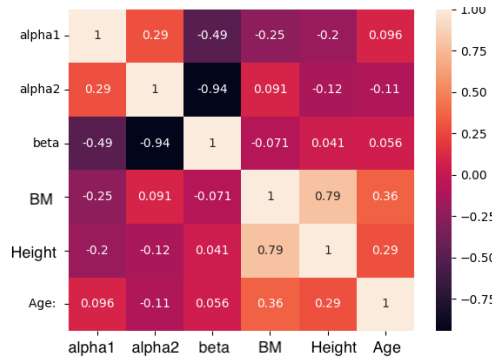


(a) Fit to raw HR

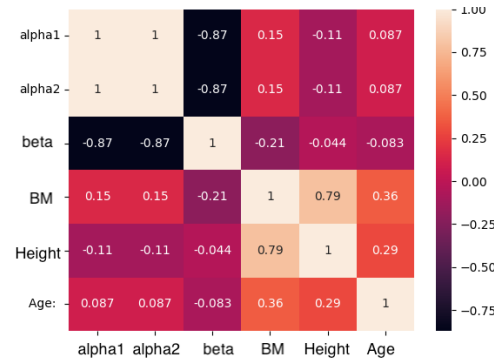


(b) Fit to smoothed HR

Figure 22: Second order linear model fit to one participant over all experiment days

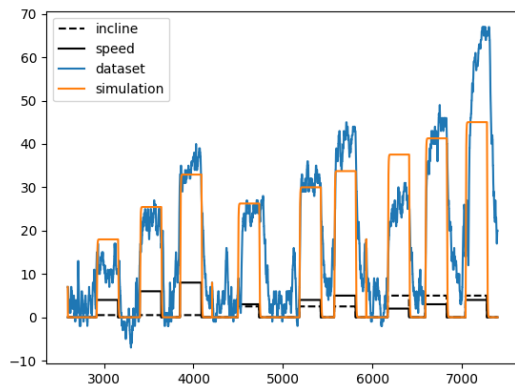


(a) Model with single input, fit to raw data

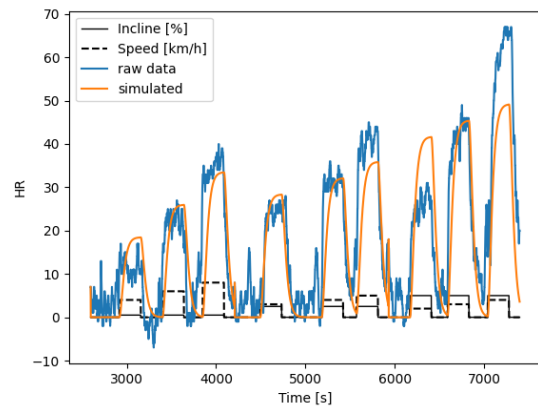


(b) Model with single input, fit to smooth data

Figure 23: Heatmap of correlations between demographic variables and parameters obtained from a second order linear model



(a) Fit to raw data



(b) Fit to smoothed data

Figure 24: Second order linear model, with input separated into two fit to one participant over all experiment days

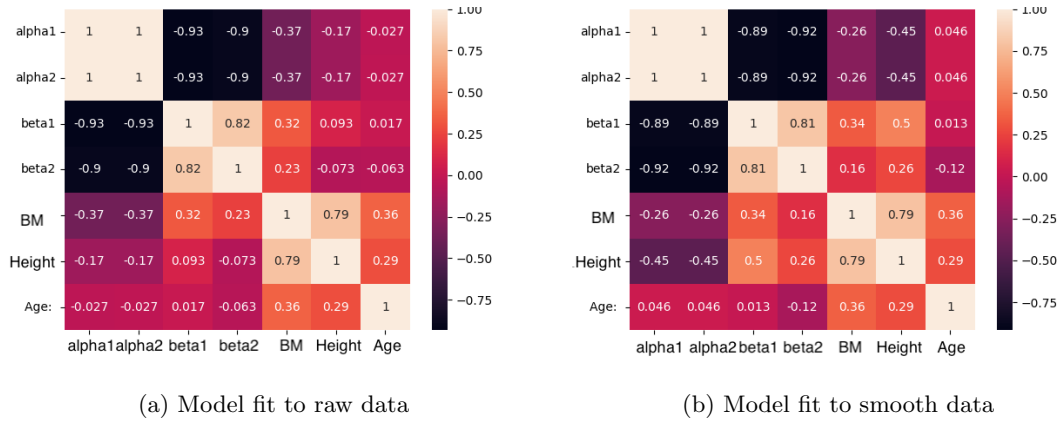


Figure 25: Heatmap of correlations between demographic variables and parameters obtained from a second order linear model with separate input

Table 4: Table of parameters and fit statistics for all models, with the optimization done on the raw HR-signal. Separated into AB and MWU and averaged over all participants. Models marked as "sep", is based on the separated input signal.

Group	Order	Model	$\alpha_1 \pm \sigma$	$\alpha_2 \pm \sigma$	$\beta \pm \sigma$	$\beta_2 \pm \sigma$	Fit $\pm \sigma$ [%]
AB	1	linear	0.97 ± 0.03	-	0.28 ± 0.16	-	26.38 ± 11.10
		linear, sep	0.85 ± 0.04	-	0.84 ± 0.04	0.85 ± 0.04	34.76 ± 12.11
		nonlinear	0.81 ± 0.22	-	0.20 ± 0.24	-	3.71 ± 11.12
		nonlinear, sep	0.91 ± 0.18	-	0.10 ± 0.18	-	44.60 ± 14.50
	2	linear	0.84 ± 0.22	0.89 ± 0.09	0.16 ± 0.21	-	22.97 ± 11.15
		linear, sep	0.88 ± 0.11	0.88 ± 0.11	0.11 ± 0.26	0.12 ± 0.21	41.08 ± 12.35
		nonlinear	0.53 ± 0.27	0.53 ± 0.27	0.27 ± 0.17	-	0.15 ± 11.17
		nonlinear, sep	0.69 ± 0.34	0.69 ± 0.34	0.2 ± 0.25	-	37.60 ± 12.24
MWU	1	linear	0.97 ± 0.01	-	0.23 ± 0.13	-	20.38 ± 16.54
		linear, sep	0.85 ± 0.03	-	0.85 ± 0.03	0.84 ± 0.04	33.13 ± 5.19
		nonlinear	0.89 ± 0.23	-	0.07 ± 0.14	-	4.2 ± 17.81
		nonlinear, sep	0.72 ± 0.28	-	0.24 ± 0.24	-	33.45 ± 15.10
	2	linear	0.88 ± 0.12	0.88 ± 0.12	0.15 ± 0.24	-	14.63 ± 9.29
		linear, sep	0.74 ± 0.12	0.74 ± 0.12	0.48 ± 0.32	0.37 ± 0.25	33.38 ± 6.55
		nonlinear	0.63 ± 0.32	0.63 ± 0.32	0.15 ± 0.14	-	-0.81 ± 20.08
		nonlinear, sep	0.55 ± 0.47	0.55 ± 0.47	0.32 ± 0.32	-	32.27 ± 16.16

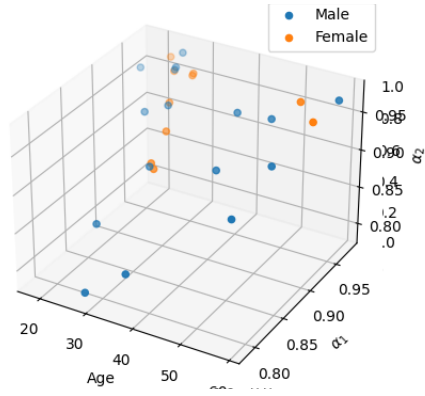
5 Discussion

5.1 Model performances

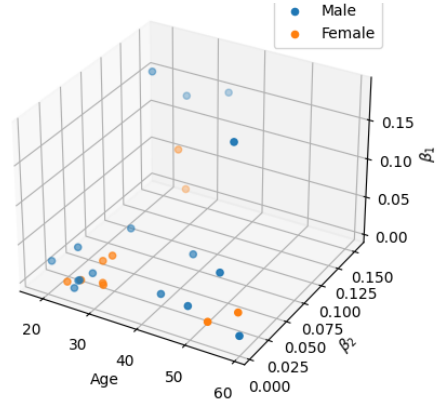
5.1.1 Input

When using the single intensity-source as input, the models consistently overestimates the HR on all the stages on the first experiment day and underestimated it for the stages on the third experiment day. They often, but not always, achieve a better fit on the second day. This is probably due to the intensity of this day being intermediate of the two others, when the optimization tries to minimize the sum of squares a trade-off has to be made between over- and underestimation of the first and third day respectively, which incidentally fits the intermediate intensity second day. The reason for the poor performance might be that the constructed input is not representative of the intensity as was the intention, there is an inverse relationship between the increase in this input and the resulting increases in HR.

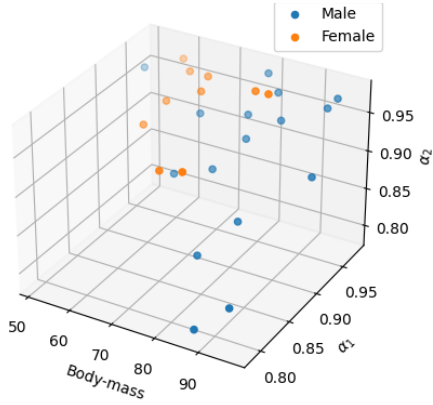
The models based on separated input consistently achieve better fit than the single input models across all orders and groups. Consequently, these models will be the focus of the following dis-



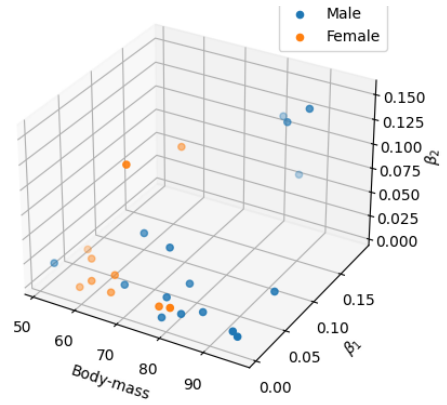
(a) Age vs. α_1 vs. α_2



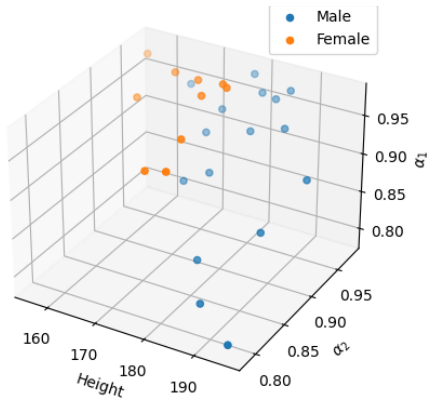
(b) Age vs. β_1 vs. β_2



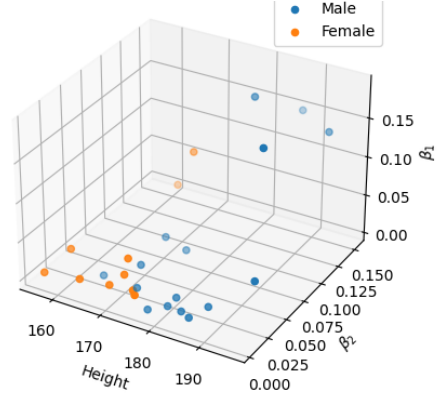
(c) Body-mass vs. α_1 vs. α_2



(d) Body-mass vs. β_1 vs. β_2



(e) Height vs. α_1 vs. α_2



(f) Height vs. β_1 vs. β_2

Figure 26: Parameters of the second order linear model, with separated input, with separated input, plotted against physical properties of each participant

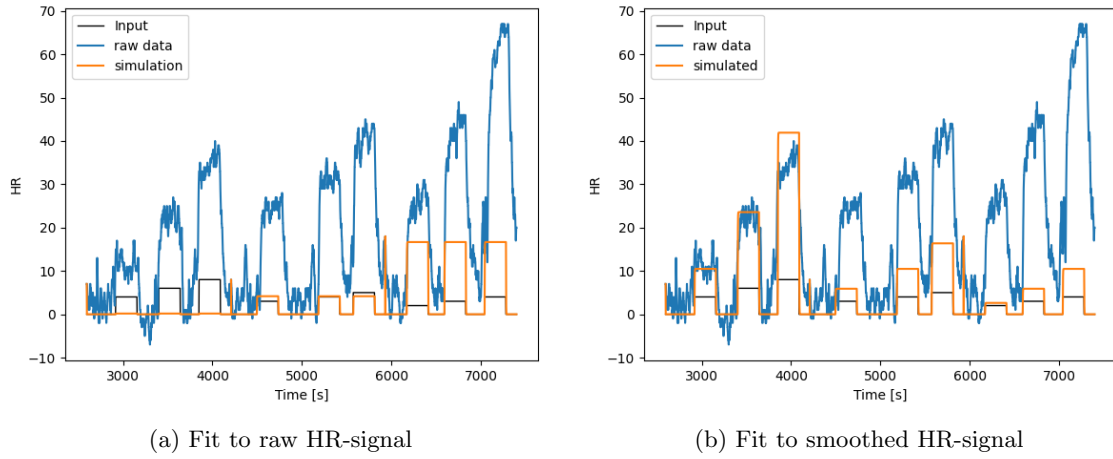


Figure 27: Second order nonlinear models fit to one participant over all three experiment days

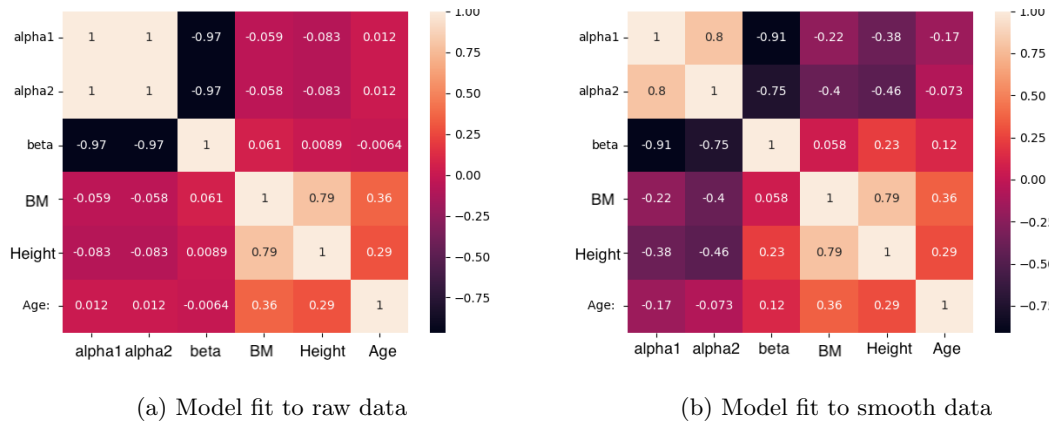


Figure 28: Heatmap of correlations between demographic variables and parameters obtained from second order nonlinear model with single input

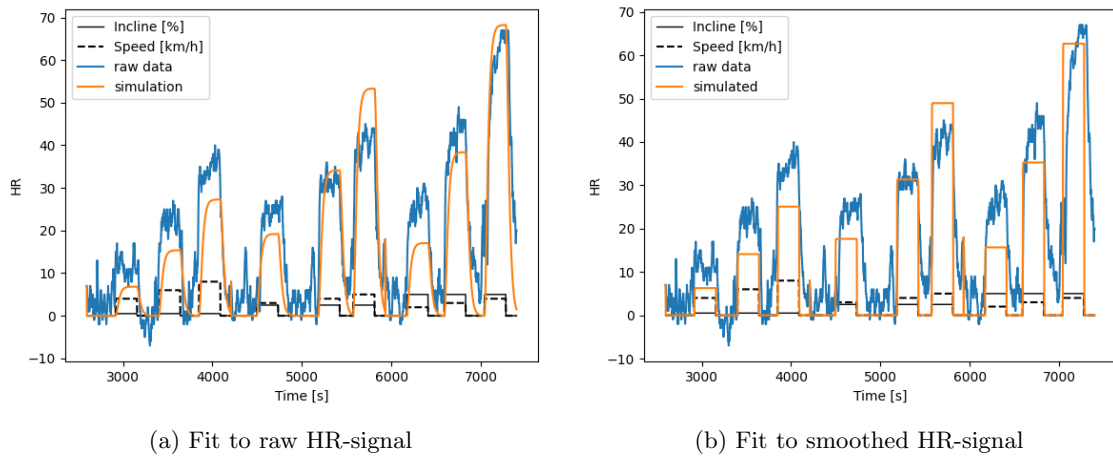


Figure 29: Second order nonlinear model, based on separated input and fit to one participant over all experiment days

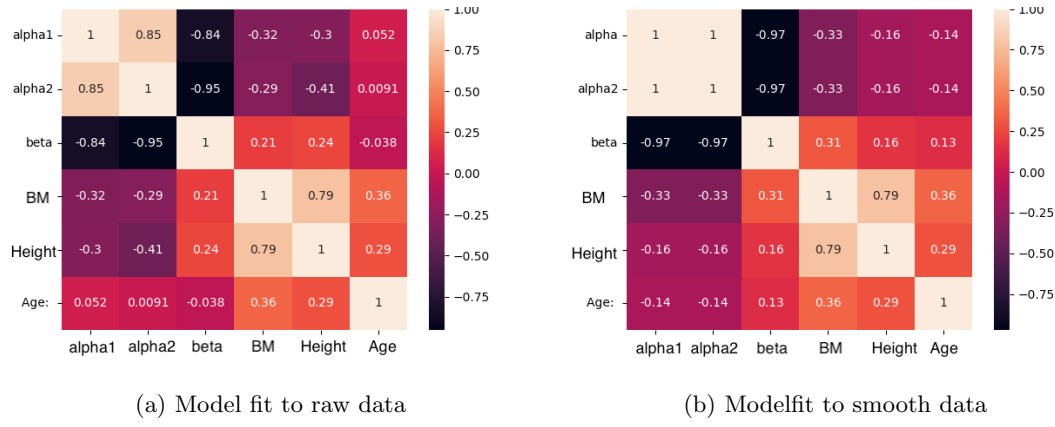


Figure 30: Heatmap of correlations between demographic variables and parameters obtained from second order nonlinear model with separated input

Table 5: Table of parameters and fit statistics for all models, with the optimization done on the smoothed version of the HR-signal. Separated into AB and MWU and averaged over all participants. Models marked as "sep", is based on the separated input signal.

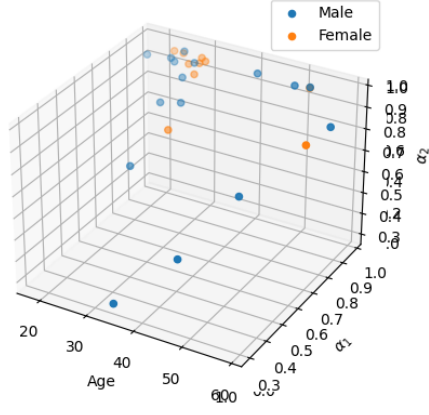
Group	Order	Model	$\alpha_1 \pm \sigma$	$\alpha_2 \pm \sigma$	$\beta \pm \sigma$	$\beta_2 \pm \sigma$	Fit $\pm \sigma$ [%]
AB	1	linear	0.98 ± 0.01	-	0.17 ± 0.09	-	23.32 ± 11.52
		linear, sep	0.98 ± 0.01	-	0.11 ± 0.05	0.13 ± 0.06	45.53 ± 10.87
		nonlinear	0.98 ± 0.01	-	0.02 ± 0.01	-	6.15 ± 10.8
		nonlinear, sep	0.98 ± 0.01	-	0.02 ± 0.01	-	46.1 ± 14.07
	2	linear	0.95 ± 0.02	0.95 ± 0.02	0.03 ± 0.04	-	22.62 ± 10.50
		linear, sep	0.92 ± 0.06	0.92 ± 0.06	0.04 ± 0.06	0.05 ± 0.05	39.71 ± 11.23
		nonlinear	0.95 ± 0.02	0.95 ± 0.02	0.003 ± 0.003	-	2.11 ± 11.08
		nonlinear, sep	0.89 ± 0.14	0.89 ± 0.14	0.03 ± 0.06	-	40.33 ± 13.35
MWU	1	linear	0.98 ± 0.01	-	0.17 ± 0.03	-	28.76 ± 12.36
		linear, sep	0.98 ± 0.01	-	0.10 ± 0.03	0.12 ± 0.06	45.06 ± 10.55
		nonlinear	0.98 ± 0.01	-	0.02 ± 0.01	-	-1.98 ± 17.9
		nonlinear, sep	0.98 ± 0.01	-	0.02 ± 0.01	-	40.54 ± 19.50
	2	linear	0.95 ± 0.02	0.95 ± 0.02	0.02 ± 0.02	-	15.311 ± 12.49
		linear, sep	0.93 ± 0.04	0.93 ± 0.04	0.05 ± 0.07	0.02 ± 0.02	36.09 ± 6.24
		nonlinear	0.65 ± 0.29	0.65 ± 0.29	0.13 ± 0.11	-	-4.74 ± 19.08
		nonlinear, sep	0.91 ± 0.13	0.91 ± 0.13	0.03 ± 0.08	-	36.59 ± 19.34

cussion. This insight is also helpful to understand which factors are necessary to derive from the wheelchair in future work. When the wheelchair is in a free living situation and not on a treadmill, gyroscopes and accelerometers can be used to derive information about speed and incline. Both of which will be important in deciding the intensity of the activity performed and thereafter the HR and EE. On a more general basis, the overall model performance might have been increased had the input been constructed in another way or been based on other intensity indicators. Further work might focus on what other parameters might be more representative as input.

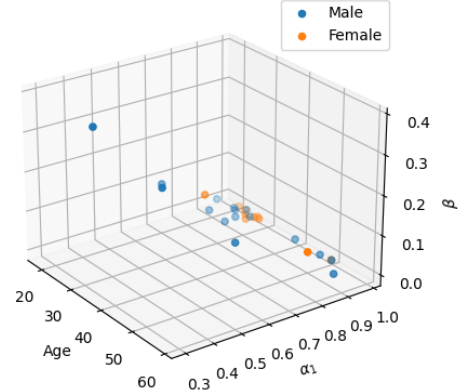
5.1.2 Order

In general the first and second order models show similar fit to the raw data, with values ranging from 36% to 46%. The standard deviations for the two are also of similar size. For the models derived from the smoothed data however, the first order models achieve marginally better fit than those of second order. The correlation-coefficient achieved with the best first order models are also higher than the ones achieved through the second order models.

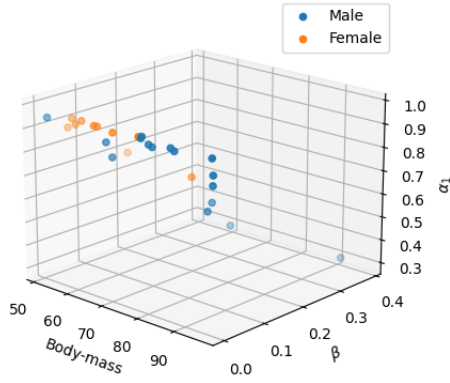
It is clear from the plots that the integrating effects that the second order models have is very



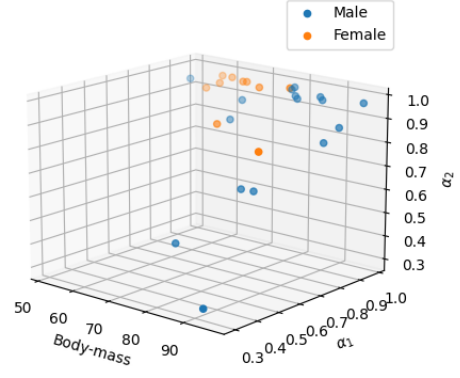
(a) Age vs. α_1 vs. α_2



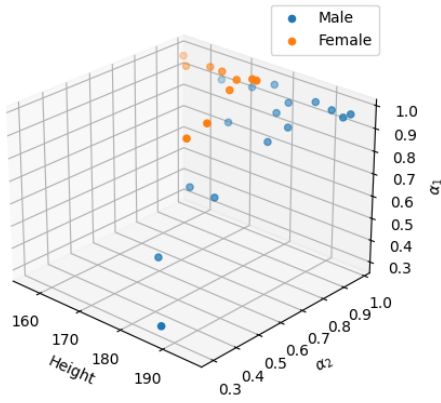
(b) Age vs. α_1 vs. β



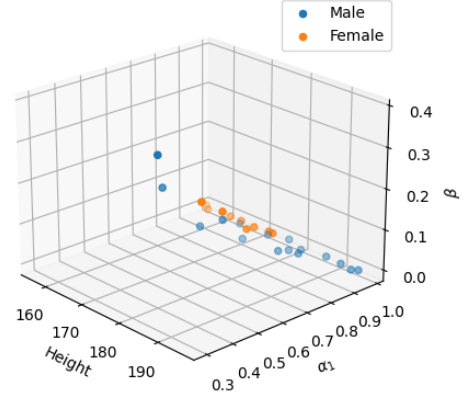
(c) Body-mass vs. α_1 vs. β



(d) Body-mass vs. α_1 vs. α_2



(e) Height vs. α_2 vs. α_1



(f) Height vs. α_1 vs. β

Figure 31: Parameters of the second order nonlinear model with separated input, based on smoothed HR-signal, plotted against physical properties of each participant

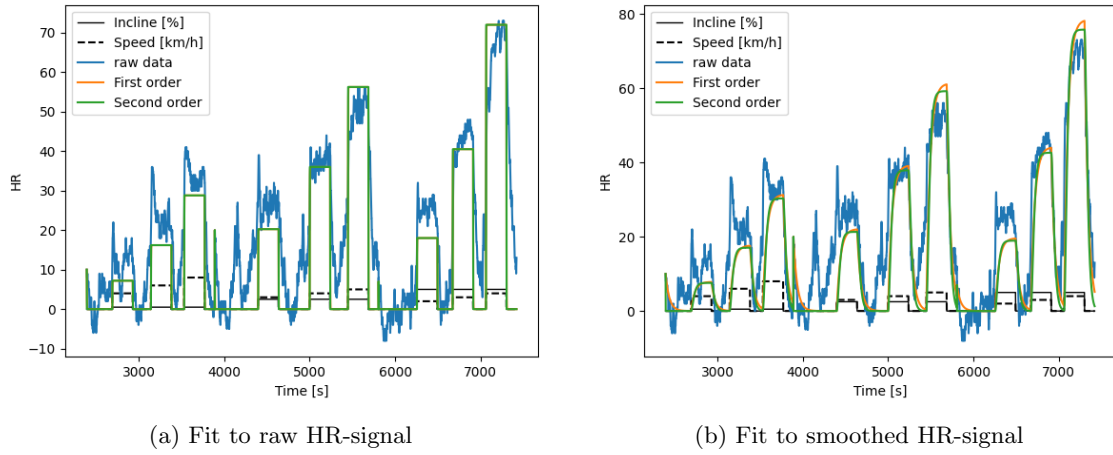


Figure 32: First and second order nonlinear model, based on separated input and fit to one participant over all experiment days. Plotted together for comparison.

small. The stages might not be long or intense enough for the participants to experience slow cardiac drift (Zakynthini, 2015). Had the participants been asked to exert themselves over a longer period, the second order models might have seen an increase in performance compared to the first order due to the fact that they might then have had more of the slow cardiac drift.

Overall, the models do not fit the data too well. There is a trend that for the highest intensities, and especially for the last stage on the third day the models underestimate the HR. First of all, this is a huge contribution to the low fit of the models. This can be verified by looking at the various plots where it is shown that the models perform very well for the lower intensities, but underestimate at the highest intensities. This might hint that there is in fact no fixed set of parameters for each individual, that they instead change when the intensity changes.

The parameters second order models consistently achieve the same parameter-values, for α_1 and α_2 , this can be seen through the correlation-coefficients having a value of 1 in the various heatmaps and in the tables 4 and 5. Since there was no prior knowledge of the parameters, they were all initialized to 0.5 which might be what caused this issue. It might also be a result of non-identifiability of these two parameters, the identifiability was not checked beforehand. If this is the case, it makes it impossible to estimate them uniquely from the given data (Guillaumea et al., 2019). Initialization of α_1 and α_2 to slightly different values in the second order nonlinear was attempted and gave slightly different results. This indicates that the problem is locally identifiable and should therefore be investigated further.

5.1.3 Linearity

An issue with the linear models was that the relationship between the increases in speed and the corresponding increases in the HR was nonlinear. The increases in HR were equal or even slightly bigger for the third day (5.0% incline), but this day had much lower speeds and much lower increases in the speeds. Thereby, making it impossible for a linear model to account for the increases in HR on the first day and last day with a linear model. Implementing nonlinearity between input and HR better captured this dynamic, as is seen through the fit statistics in the table 4 and 5. The nonlinear model identified here squared the speed and multiplies it by the incline. This indicates that the HR-increase based on a speed increase is highly dependent on the incline it is performed at and reinforces the need for a non-linear model.

Table 6: IPAQ correlations between AB-participants and parameters of different models, averaged over all AB participants

Model	Linearity	Input-type	Data	α_1	α_2	β_1	β_2
First order	Linear	Single	Raw	0.004	-	0.004	-
			Smooth	0.023	-	-0.13	-
		Separated	Raw	-0.11	-	-0.11	-0.078
			Smooth	-0.18	-	0.12	-0.33
	Nonlinear	Single	Raw	0.22	-	-0.19	-
			Smooth	-0.17	-	-0.051	-
		Separated	Raw	0.22	-	0.019	-
			Smooth	-0.27	-	0.051	-
Second order	Linear	Single	Raw	-0.11	0.10	-0.09	-
			Smooth	-0.23	-0.23	0.1	-
		Separated	Raw	-0.16	-0.16	0.057	0.045
			Smooth	-0.21	-0.21	0.26	0.15
	Nonlinear	Single	Raw	-0.13	-0.22	0.18	-
			Smooth	0.0	0.31	-0.30	-
		Separated	Raw	-0.09	-0.09	0.07	-
			Smooth	0.31	0.31	-0.3	-

5.1.4 Smoothing

Overall the models that were generated from the smoothed data achieved better fit, this can be seen through comparison of table 4 and 5, from the plots of the models it can also be seen that they followed the shape of the HR to a better extent. The standard deviations were of similar order. When basing the model on the smoothed data the residuals are a better estimate of the lack-of-fit of the model. In the raw data, certain residuals will be large by virtue of the noise, and not necessarily poor model performance. Thus, the numerical optimization might obtain better models from less noisy data. Whereas the dynamics obtained from the raw signals often are too fast compared to the actual, due to the influence of the noise. The resulting dynamics from the smoothed data were naturally slower with longer time constants, as a consequence of the removal of the fastest frequencies from the signal. The slower dynamics derived from these models were likely more descriptive of the actual dynamics as they provided stronger correlations with the physical characteristics as can be seen by comparing the heat-maps provided in the results.

It is arguable, however, that the smoothing-method did not preserve physiological properties. The fluctuations in the HR signal may not only be due to noise, HR measured in bpm tends to have non-stochastic spontaneous fluctuations that may have biological significance (Zakynthini, 2015). Thus, removing them from the process may be problematic in terms of the physiological implementations.

5.1.5 Generalizability

The optimized parameters were similar between the AB group and the MWU group as can be seen in tables 4 and 5. Moreover, in the cases where they are slightly different, they still lie within the range of each others standard deviations. This indicates that there is a good possibility for generalizing from AB-data to MWU-data. On the other hand, the models often had a worse performance on the MWU and higher standard deviations compared to the AB, which is a reflection of the heterogeneity of the group. Overall the standard deviations of the parameters were significantly large, which reiterates the need for individualization of the models.

5.2 Demographic correlations

The correlations found between the different demographic variables and the obtained parameters can be classified as low to moderate. However, they do yield some possibilities for individualizing the model based on weight and height. Especially, the first order models based on smoothed data showed negative correlations around 0.5 between the body-mass, height and optimized parameters. Several of the models, showed body-mass as negatively correlated with β . This indicates that the higher the body mass is the lower will the steady-state gain from the input be.

The three-dimensional plots show that there are outlines of gender based clusters which may allow for gendered grouping of the parameters. In the first order nonlinear model we saw that the women generally had higher β than the male participants. This indicates that the input is more important in determining their HR than it is for the male, giving them higher steady-state gain.

Some of the models showed a weak correlation between IPAQ value and the α parameter as can be seen in 6. The correlation was in most cases negative, indicating a decrease in α with increase in IPAQ-score. Consequently, the models showed that the higher the IPAQ score, indicating higher PA levels in daily life, gave a higher time-constant and thereby slower increase of HR. The correlation was not calculated between the MWU and IPAQ since the specific answers for this group were not accessible. The only available information of the IPAQ-values was that all MWU fell into the highest IPAQ-category, which was not useful for correlation calculations. On the other hand the validity of IPAQ as a metric for scoring physical activity-levels for MWU has not been sufficiently investigated in the existing literature. Thereby, using this for comparing AB and MWU in the same manner, might not be appropriate regardless.

5.3 Challenges

There were many challenges with the data-collection, the main, as previously discussed being the falling-out of sensors. Moreover, several different persons have been involved in the data-collection and the standardization of procedure was not set from the start, causing discrepancies from the current procedure. A lot of time and effort had to be put into making a pipeline from raw HR-signal to a useful signal that worked for all participants. There were a lot of variances to account for and special unforeseen cases. Another challenge was that the MWU data was recorded continuously throughout the process of writing the thesis. Thereby, new special cases had to be accounted for throughout rendering the previous pipeline insufficient. As of the finalization of the work on this thesis, the pipeline is still not perfect. Therefore, many of the MWU participants data had to be left out and there are still some participants where the resulting dataset is not perfectly put together, which is likely the cause of the outliers seen in the results.

It is also valuable to highlight the challenges with constructing mathematical models on biological features of humans. There exists huge biological variations between individuals, meaning that there might not be a standard model that works for all. Moreover, the participants were all tested in similar physical states as enforced by the requirements, a single individual's dynamics might vary with time of day, eating, stress and so on. There are many factors affecting each other in the body creating complicated responses and abstracting to the level we have here might make it difficult to capture the essential features. The measurements of all physiological aspects of the processes happening inside the body is difficult, especially without invasive methods and sensor measurements. Furthermore, the measurements are subject to noise due to the intrinsic properties of measurement on the human body.

5.4 Further research

There is a huge potential for further research on the topics regarded in this thesis. A short list is given below.

-
- Using the identified models to further identify a model for the estimation of energy expenditure for manual wheelchair users
 - Attempt to identify a model where the dynamics change at a certain intensity level, either in the form of a change of order, or another structure alteration.
 - Implement of a model with different time-constants for the raise and fall of HR.
 - Investigate the possibilities of developing online HR trackers and individualize the model structures based on personal characteristics.
 - Investigate the identifiability of the models.
 - Investigate the performance of second order models with different parameter-initializations.

6 Conclusion

This thesis investigated the development of mathematical models for estimating heart rate during wheelchair propulsion. Speed and incline of the movement on the treadmill were defined as the inputs to the dynamical system. System identification and numerical optimization were used to find the best structure and the corresponding parameters.

Evaluating the estimation results indicates that both speed and incline is needed to generate useful input to estimate heart rate. Moreover, there is a nonlinear relationship between the speed and incline as input and the HR as output. The performance of the models did not increase when extending them from the first to the second order. However, this might be a result of the activity bouts being too short to generate slow-cardiac response or the initialization of parameters. Smoothing the HR-signal provided models with better fit and showed stronger correlations with the demographic information on the participants. It is important not to draw too strong conclusions from this though, as some of the physiological aspects of HR were lost in the smoothing process. The optimized parameters and fit showed that generalizability from AB to the more heterogeneous group of MWU is viable, despite slightly higher variation in the results. The correlations found between parameters and demographic variables were not strong, but give some indications as to which variables might be useful in an individualization of the model, these were: body-mass, height and gender. Some correlations were shown with IPAQ factor, but no conclusions can be drawn here with regards to the MWU-group as there was a lack of data in this respect.

In conclusion; although not perfect, a first order nonlinear model provided both the best fit, the strongest correlations and the best opportunity of grouping based on gender.

References

- Andresen, Trond, Jens G. Balchen and Bjarne A. Foss (2016). *Reguleringsteknikk*. Institutt for teknisk kybernetikk.
- Borg, G. A. (1982). 'Psychophysical bases of perceived exertion'. In: *Med Sci Sports Exerc* 14.5, pp. 377–81.
- Cappozzo, Vittoria (2022). 'Modeling and identification of heart rate and energy expenditure dynamics for manual wheelchair users'. Universita Degli Studi di Padova.
- Collins, E. G. et al. (2010). 'Energy Cost of Physical Activities in Persons with Spinal Cord Injury'. In: 42, pp. 691–700.
- Disease Control, Centers for and Prevention (2022). *What is Cerebral Palsy?*
- Guillaumea, Joseph H.A. et al. (2019). 'Introductory overview of identifiability analysis: A guide to evaluating whether you have the right type of data for your modeling purpose'. In: *Environmental Modelling Software* 119, pp. 418–432.
- Hauser, Raphael (2005). *SECTION: CONTINUOUS OPTIMISATION, LECTURE 4: QUASI-NEWTON METHODS*. <https://www.numerical.rl.ac.uk/people/nimg/oupartc/lectures/raphael/lectures/lecture4.pdf>.
- I.M., Majer et al. (2011). 'Mortality risk associated with disability: a population-based record linkage study.' In: *Am J Public Health*. 101, p. 12.
- IPAQ, Research Committee (2004). *Guidelines for Data Processing and Analysis of the International Physical Activity Questionnaire (IPAQ) - Short Form*. https://www.physio-pedia.com/images/c/c7/Quidelines_for_interpreting_the_IPAQ.pdf.
- Kesaniemi, Y. Antero et al. (2001). 'Dose-response issues concerning physical activity and health: an evidence-based symposium'. In.
- Khemila, S. et al. (2022). 'The effect of time of day and high intensity exercise on cognitive performances of elite adolescent karate athletes'. In: 39.12. 10.1080/07420528.2022.2132165, pp. 1542–1553.
- Kirshblum, Steven C. et al. (2011). 'Reference for the 2011 revision of the international standards for neurological classification of spinal cord injury'. In: 34.6, pp. 547–554. DOI: 10.1179/107902611X131860004202425.
- Moreno, Daniel et al. (2020). 'Validity of Caloric Expenditure Measured from a Wheelchair User Smartwatch'. In: *International Journal of Sports Medicine* 41.08, pp. 505–511.
- NHS (2022). *Ehlers-Danlos syndromes*.
- Nightingale, T.E., P.C. Rouse and D. Thompson et al. (2017). 'Measurement of Physical Activity and Energy Expenditure in Wheelchair Users: Methods, Considerations and Future Directions.' In: 3. <https://doi.org/10.1186/s40798-017-0077-0>, p. 10.
- Nocedal, Jorge and Stephen J. Wright (2006). *Numerical Optimization, Second Edition*. Springer Science+Business Media.
- Organization, World Health (n.d.). *Guidelines on the provision of Manual Wheelchairs in less resourced settings*. <https://apps.who.int/iris/bitstream/handle/10665/205041/B4616.pdf?seq>.
- Osgood, Brad (2007). *Lecture Notes for EE261 The Fourier Transform and its Applications*. URL: <https://see.stanford.edu/materials/lsoftae261/book-fall-07.pdf>.
- Paluska, S.A. and T.L. Schwenk (2000). 'Physical activity and mental health: current concept'. In: 29. <https://pubmed.ncbi.nlm.nih.gov/10739267/>, pp. 167–180.
- Patel, Parth N. (2022). 'Physiology, Exercise'. In.
- Sorenson, H. W. (1970). 'Least-squares estimation: from Gauss to Kalman'. In: *IEEE Spectrum* 7.7, pp. 63–68. DOI: 10.1109/MSPEC.1970.5213471.
- Tsang, KaLai et al. (2017). 'Validity of activity monitors in wheelchair users: A systematic review'. In: 3. <https://doi.org/10.1186/s40798-017-0077-0>, p. 10.
- Walpole, Ronald E. et al. (2016). *Probability & Statistics for Engineers & Scientists*. Pearson Education Limited.
- Warm, Catherine A., JoAnne D. Whitney and Basia Belza (2008). 'Measurement and description of physical activity in adult manual wheelchair users'. In: *Disability and Health Journal* 1.4, pp. 236–244.
- Weil, Evette et al. (2002). 'Obesity among adults with disabling conditions'. In: *Jama* 288.10, pp. 1265–1268.
- Zakynthinaki, Maria S. (2015). 'Modelling Heart Rate Kinetics'. In: *PLoS ONE* 10.4.

Zhu, Ciyou et al. (Dec. 1997). ‘Algorithm 778: L-BFGS-B: Fortran Subroutines for Large-Scale Bound-Constrained Optimization’. In: *ACM Trans. Math. Softw.* 23.4, pp. 550–560. ISSN: 0098-3500. DOI: 10.1145/279232.279236. URL: <https://doi.org/10.1145/279232.279236>.